NASA CONTRACTOR REPORT

NASA CR-2891

NASA CR-2891

GRAVSAT/GEOPAUSE REFRACTION STUDY

S. K. Llewellyn, et al.

Prepared by
ATLANTIC SCIENCE CORPORATION
Indialantic, Fla. 32903
for Goddard Space Flight Center

NATIONAL AERONAUTICS AND SPACE ADMINISTRATION • WASHINGTON D. C. • AUGUST 1977

1. Report No.	2. Government Accession No.	3. Recipient's Catalog No.
NASA CR-2891		

4. Title and Subtitle	5. Report Date
GRAVSAT/GEOPAUSE Refraction Study	August 1977
	6. Performing Organization Code
7. Author(s) S. K. Llewellyn, et al.	8. Performing Organization Report No.
9. Performing Organization Name and Address Atlantic Science Corporation, P. O. Box 3201, Indialantic, Florida 32903	10. Work Unit No.
	11. Contract or Grant No. NAS 5-20744
	13. Type of Report and Period Covered
12. Sponsoring Agency Name and Address National Aeronautics & Space Administration, Washington, D. C. 20546	
	14. Sponsoring Agency Code

15. Supplementary Notes

16. Abstract

A refraction study was performed for the following GRAVSAT/GEOPAUSE configuration; a ground station network was tracking a high altitude spacecraft, and this spacecraft was in turn tracking a low orbiting satellite and relaying the orbit data to the ground stations. New techniques were developed for computing ionospheric and tropospheric refraction effects along the satellite link, and the existing NASA/Worldwide Refraction Model was utilized to compute the corrections for the ground link. Tests were performed demonstrating severe refraction conditions. The maximum one-way ionospheric errors were determined as 2.6m in range and 17 mm/sec in range-rate for the satellite leg at frequencies of 13.5 GHz. Maximum tropospheric errors for range and range-rate respectively amounted to 260m and 23 m/sec along the satellite link as the ray passes close to the earth's surface, and to 130m and .5m/sec along the ground link.

17. Key Words (Selected by Author(s))	18. Distribution Statement
Refraction Satellite tracking	Unclassified - Unlimited

19. Security Classif. (of this report)	20. Security Classif. (of this page)	21. No. of Pages	22. Price*
Unclassified	Unclassified	64	$4.50

*For sale by the National Technical Information Service, Springfield, Virginia 22161.

TABLE OF CONTENTS

LIST OF FIGURES

LIST OF TABLES

1.0 INTRODUCTION

NASA/GSFC envisions the use of low orbiting spacecraft, like the GRAVSAT satellite, for purposes of scientific explorations. These spacecraft are to be tracked by a high altitude GEOPAUSE satellite acting in a relay capacity. In order to fulfill the mission objectives of this satellite-to-satellite configuration the required tracking accuracies are of the order of 0.02 meters in range and 0.003 cm/sec in range-rate.

To optimize the GEOPAUSE system, trade-offs will have to be made between tracking frequencies, orbits, station locations and scheduling of times during which tracking should be performed.

One of the important factors affecting the achievement of these accuracy specifications is the refraction effects produced by the earth's ionosphere and troposphere to the radio tracking signal. A study was thus necessary to define the limitations on system performance expected to be imposed by the presence of the earth's atmosphere. The study considered a range of tracking frequencies between 2GHz and 15GHz and a number of satellite-to-satellite configurations for polar orbits. The ground tracking stations considered are in the existing NASA network.

The ionospheric and tropospheric effects were computed from the NASA/Worldwide Model as it exists in the GTDS program, utilizing Marini's tropospheric equations and the Bent ionospheric model.

2.0 RESULTS FROM PREVIOUS REFRACTION STUDIES

When a high orbiting satellite tracks a lower orbiting satellite and the line of sight between the two passes through a refracting medium the signals will be subject to retardation. This retardation will be greater for situations where the line of sight passes almost tangentially to the earth's surface. With this configuration, it may pass through two ionospheres and effectively two tropospheres. At times, it may also pass along the height of maximum electron density for considerable distances causing an effective total electron content of well over $10^{19} e/m^2$ column. Obviously at these times, the tracking problems can be serious and hence corrections must be made.

For the Tracking Data Relay Satellite System (TDRSS) a number of orbits had been investigated that exhibited extreme ionospheric refraction situations. The initial correction technique that was developed for the satellite-to-satellite link had successfully demonstrated the significant errors that can exist in the range measurements. It also had pointed out specific problems that were encountered in computing range-rate corrections through the ionosphere.

Many Doppler satellite tracking systems integrate cycle counts over a few seconds of time. The ionospheric corrections for such a technique are best obtained by range differencing the ionospheric corrections and dividing by the integration period, thus automatically incorporating the variations due to changes in time, elevation, azimuth and height. A typical ionospheric range-rate correction can be significantly changed by the sixth digit in the ionospheric range correction when differencing, which puts an extremely high requirement on the consistency with which the refraction in range is computed. No irregularities are allowed in calculating the two adjacent range corrections, and in the numerical integration the errors at the interfaces between the different electron density layers have to be overcome. The ionospheric height at the ray intersection point must be computed to 1 km convergence in order to obtain a precise ionospheric latitude and longitude for $f_o F2$ computations. An error of over 1 km in $h_m F2$ will cause the $f_o F2$ value to be very slightly different, which could easily modify the 5th or 6th digit in range leading to very large errors in range-rate. It is not claimed that $h_m F2$ has to be accurate to 1 km as this is an impossible prediction, but the values of $h_m F2$ should be consistent in their calculation to 1 km convergence.

These problems have been previously overcome by choosing very small intervals along the raypath at which the ionosphere was recomputed, and then numerically integrating over all refraction contributions. This approach was not practical for applications though, since it required a prohibitive amount of computer time. Thus, based on the knowledge of the particular difficulties in computing range-rate corrections, a completely new correction technique was developed for the GRAVSAT/GEOPAUSE satellite system yielding the required accuracies and minimizing the computer time.

3.0 TECHNIQUE FOR REFRACTION CORRECTIONS ALONG THE GROUND-TO-SATELLITE LINK

The NASA tracking network is comprised of 6 ground stations for this project, 3 in the northern and 3 in the southern hemisphere. These stations were selected based on their ability to provide continuous global tracking of the GEOPAUSE during its tracking GRAVSAT, and they are Guam, Madrid, Rosman, Canberra, Johannesburg and Santiago. Whenever the GEOPAUSE satellite is visible from any of the tracking sites, the refraction corrections to range and range-rate for that link are computed from the NASA/Worldwide Model as it exists in the GTDS program.

The tropospheric corrections to range ΔR_T are computed using Marini's model (Reference 1). The range-rates $\Delta \dot{R}_T$ are computed by range differencing over a 10 second interval,

$$\Delta \dot{R}_T \ (t) = \frac{\Delta R_T \ (t + \Delta t) - \Delta R_T \ (t)}{\Delta t} . \qquad (3-1)$$

The refractivities and scale heights on which the refraction computations are based are a fixed set of monthly values for each station.

The ionospheric corrections to range ΔR_I are calculated using the Bent ionospheric profile model (Reference 2), and are based on an overall transmission frequency f in Hertz, giving

$$\Delta R_I = \frac{40.3 \ N_T}{f^2} , \qquad (3-2)$$

where N_T is the total electron content along the angular path in electrons/ m^2 column, and the range correction is in meters. The frequency is computed in terms of the uplink and downlink frequencies f_u and f_d,

$$\frac{1}{f^2} = \frac{1}{2} \left(\frac{1}{f_u^2} + \frac{1}{f_d^2} \right) . \qquad (3-3)$$

The range rates $\Delta \dot{R}_I$ are computed by range differencing over a 10 second interval,

$$\Delta \dot{R}_I \ (t) = - \frac{\Delta R_I \ (t + \Delta t) - \Delta R_I \ (t)}{\Delta t} . \qquad (3-4)$$

4.0 TECHNIQUE FOR REFRACTION CORRECTIONS ALONG THE SATELLITE-TO-SATELLITE LINK

New techniques had to be developed to compute the corrections to range and range-rate tracking observations that compensate for tropospheric as well as ionospheric refraction effects along the satellite-to-satellite communication link. It was taken under consideration to achieve the accuracies as required and to formulate the algorithms in such a fashion that the computer time necessary to do the calculations would remain reasonably low for application purposes.

4.1 Tropospheric Corrections for the Satellite-to-Satellite Link

In the satellite configuration under investigation the low satellite is considered to be in a 300 km high circular orbit. Since the tropospheric refraction occurs at low altitudes and is negligible at heights above about 90 km, tropospheric errors will be introduced into the tracking data only at times when the raypath between the satellites gets close to the earth's surface. These conditions are rarely met, and happen only within approximately the first and last 30 seconds of each pass when the low satellite appears or disappears from the sight of the high satellite, see Figure 1.

To compute the refraction effects for these cases, a modified version of the standard tropospheric program was employed. Marini's model requires as known information the refractivity and scale height of the surface point, and the elevation angle at which the raypath terminates for ordinary ground-to-satellite communications. For the satellite-to-satellite link however, there will be no intersection with the ground whenever tropospheric effects exist, and the point along the raypath that defines the closest approach to the earth takes on the significance of the ground point. For this point at height h the refractivity N is computed from the wet and dry components N_d and N_W of the surface refractivity vertically below by,

$$N(h) = N_d e^{-\frac{h}{H_d}} + N_W e^{-\frac{h}{H_W}} . \qquad (4\text{-}1)$$

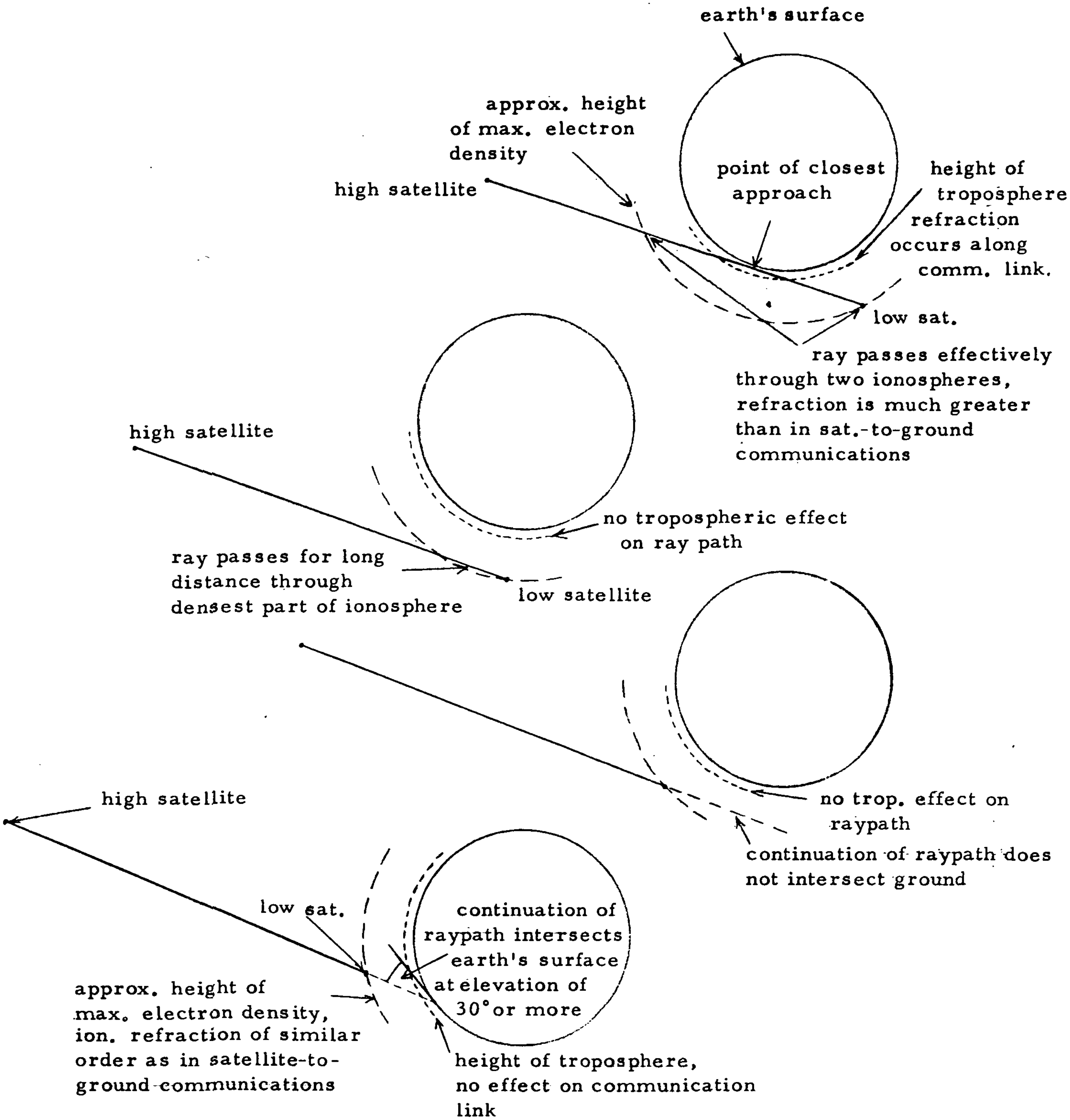

Figure 1. Illustration of Various Satellite Configurations Relative to Troposphere and Ionosphere

The scale height components H_d and H_w are the same as for the surface point and combine to the total scale height value H as,

$$H = \frac{H_d N_d + H_w N_w}{N_d + N_w} \quad . \qquad (4\text{-}2)$$

An elevation angle of 0 degrees is assumed, since the raypath runs tangential to an imaginary shell at a distance h out from the earth's surface. The tropospheric calculations for the range correction were based on these values of refractivity, scale height and elevation angle, and the result was multiplied by two, to account for refraction between the satellites to both sides of the point of closest approach. Range-rate corrections were obtained by range differencing, the same as in the equation (3-1).

Since it is a very rare situation to encounter tropospheric refraction along the satellite link during the specified orbits, no extended effort was put into modeling the refractivity and scale height data on a worldwide basis. Instead a very simple model was used that interpolated for the required latitudes between the values listed in the table below for artic, temperate and tropic latitudes.

Latitude	N_d	N_w	H_d	H_w
artic - 79°	332	1	6.3	6.5
temperate - 39°	266	59	9.0	2.5
tropic - 3°	259	112	9.4	2.0

This approach of computing tropospheric corrections is reasonable, because the range corrections for sample cases when the point of closest approach was at heights of 0 and 80 km were of ratios similar to those for the refractivity values at the same heights. Tests were performed to examine the total range of correction values that can be obtained from this simple model at any geographic location. Figures 2 and 3 show the possible values for the tropospheric range and range-rate corrections along the satellite-to-satellite link. They are plotted against the time

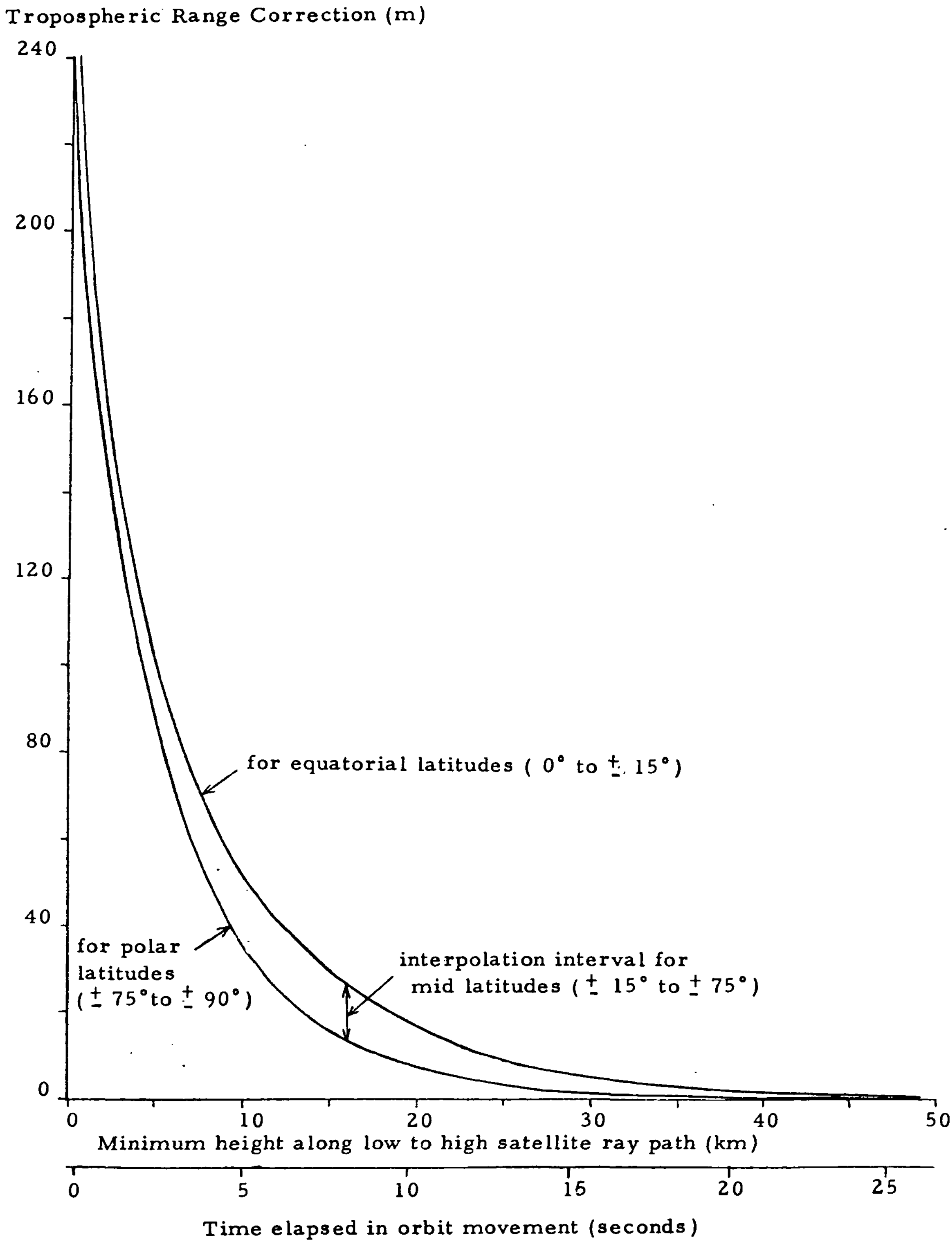

Figure 2. Tropospheric Range Corrections for Satellite-to-Satellite Link and Associated Time Interval

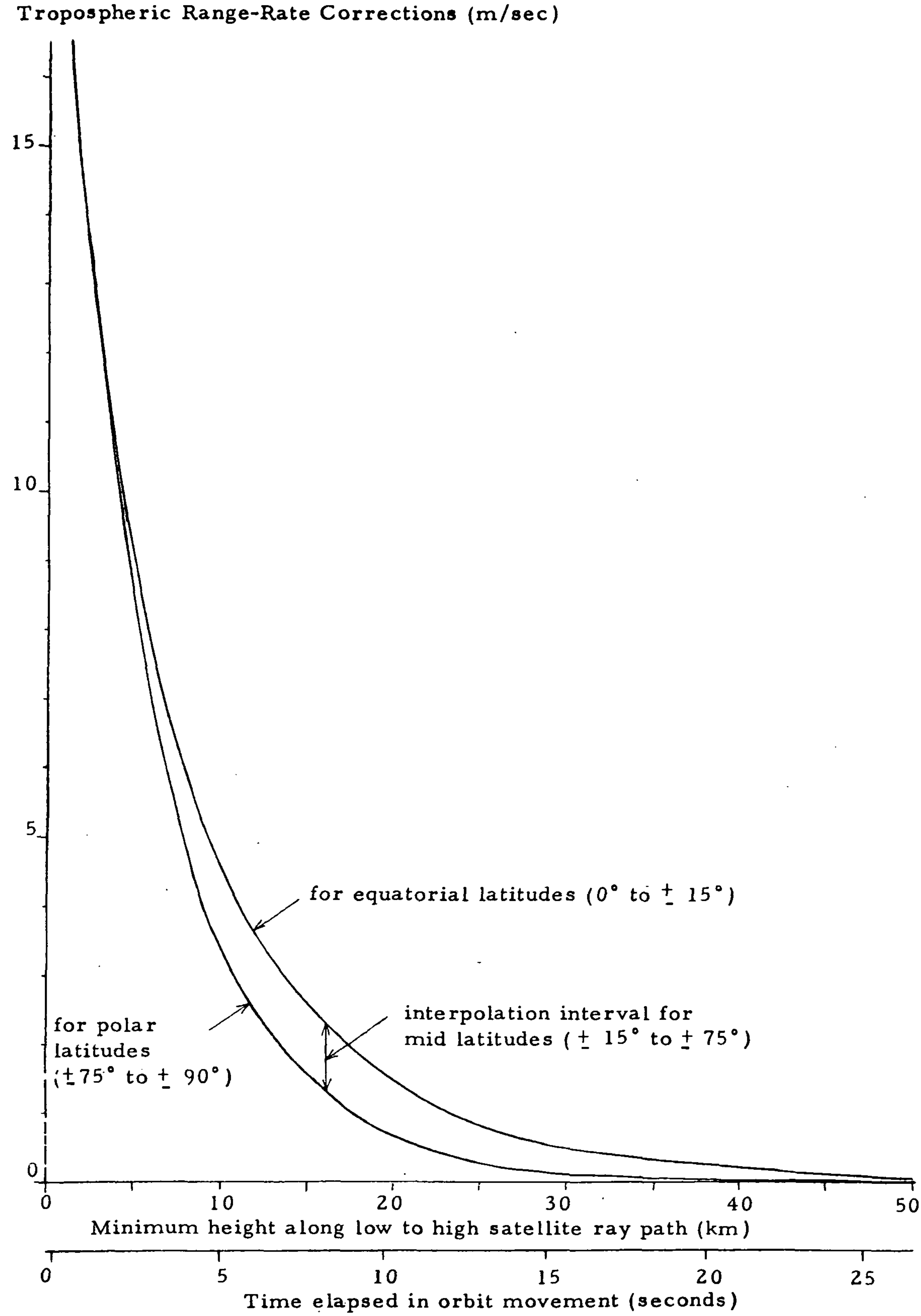

Figure 3. Tropospheric Range-Rate Corrections for Satellite-to-Satellite Link and Associated Time Interval

elapsed in the orbit movement from the first visible point, and also against the height along the raypath that defines the point of closest approach to the earth.

4.2 Ionospheric Corrections for Satellite-to-Satellite Link

Depending on the relative satellite positions,one of two different methods was utilized to compute the ionospheric refraction incurred along the satellite-to-satellite leg. Corrections are based on single profile computations using the standard model whenever the slant of the raypath was not extreme, because the required computer time is kept low while the accuracy achieved is good. For very slanted paths however, this approach was not satisfactory, and corrections were based on a number of profile computations along the path. The geometry of several typical satellite configurations is shown in Figure 1, where the last situation is an example of the following category. For any case in which the continuation of the satellite connecting line past the low satellite intersects the surface of the earth at a ground elevation angle of 30 degrees or more, the standard ionospheric refraction method is utilized. The satellite-to-satellite range correction is the difference between the range corrections from ground up to the high and low satellites, which are computed as closed form solutions with the Bent model.

ΔR (low to high sat.) = ΔR (ground to high sat.) - ΔR (ground to low sat.)

The range-rate corrections were again based on consecutive range corrections and calculated as in equation (3-4).

Whenever the satellite connecting line and its continuation stayed above the earth's surface or whenever it formed a ground elevation angle of less than 30 degrees, another method was applied. Along these slanted paths the ionospheric spacial gradients can be very large, and to maintain the required accuracies, recomputation of the refraction effects at a number of points along the path is necessary, ruling out a closed form solution. A new technique was developed for computing the ionospheric refraction at strategic points along the path from the low to the high satellite. A cubic spline interpolation was selected to fit additional values into the intervals between points at the locations specified by the Gaussian quadrature method which is used for numerically integrating the computed electron density values over the distance from the low to the high satellite. The 30 degree ground elevation situation was selected for switching from the closed form to the numerical method after a series of tests had been performed. As shown in Figure 4, applying the closed form standard model down to the 0 degree elevation point introduces significant inconsistencies in the range corrections where the different methods interface, while switching methods at 30 degrees elevation insures a smooth transition.

Many different aspects were investigated in the development of a technique for computing satellite-to-satellite ionospheric corrections. The spacing of points at which the electron densities were calculated along the direct path connecting the satellites was modified many times, to arrive at the best selection for which the number of points would be low, and yet the accuracy specifications could be met even under extremely high refraction conditions. For a smooth numerical integration many additional points between the accurately computed ones were necessary, and these were obtained by fitting various curves through the electron density values as a function of distance. Calculating these many points directly from the ionospheric model rather than from the fit would have involved too much computer time and was therefore only done to verify test results. Polynomial fits were found to be altogether unsatisfactory in terms of accuracy achieved, and after a number of tests a cubic spline interpolation was selected as the best choice. The problems in the numerical interpolation through all electron densities from low to high satellite had been pointed out in previous work, where trapezoidal integration and Simpson's rule had been viewed with reservation because of the great amount of computer time involved and the accuracy problems. For this reason, the Gaussian quadrature method was investigated which gave very satisfactory results.

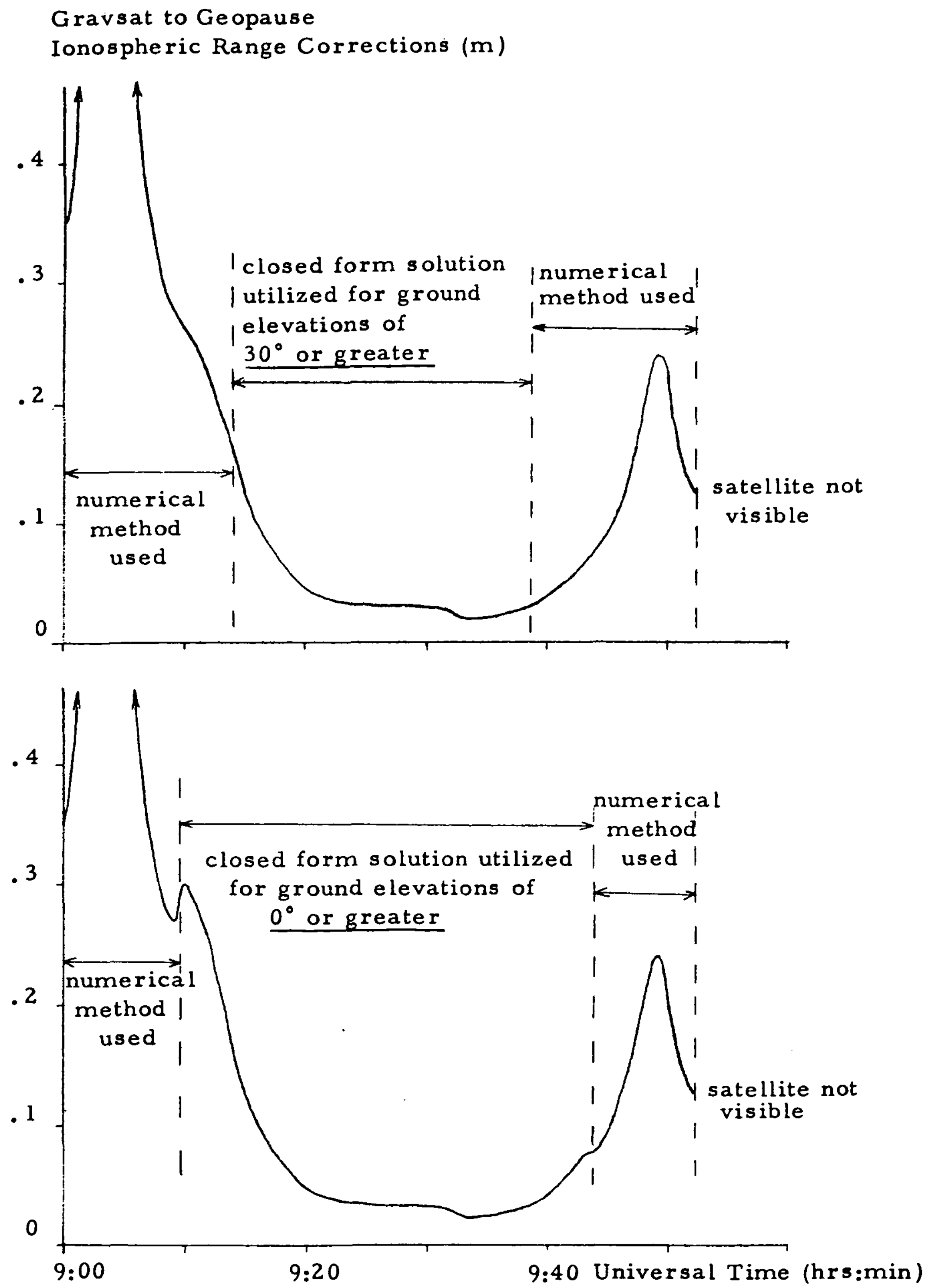

Figure 4. Transition in Range Corrections for Switching from Numerical to Closed Form Method at 30° and 0° Ground Elevation

Point Selection

Since the spline interpolation, through which extra points are added into the gaps, accepts points at irregular intervals, the freedom existed to choose points at preferred locations and uneven spacing.

The first point was thus selected in the region where the most significant portion of electrons is encountered, at the intersection of the raypath and the height of maximum electron density. This location is used as a reference point on which the selection of other points is based. As a first estimate the reference point is computed assuming a height of maximum density at 300 km, whenever the geometry shows the satellite connecting ray to pass within 300 km or less of the earth's surface. Using this estimate the height of the maximum is computed and then interated on yielding the new height value to within 1 km convergence along with the corresponding electron density profile parameters. If however, the raypath always remains at a greater distance from the earth's surface, the first height estimate is increased in 25 km steps up to a maximum value of 450 km. In the cases when the raypath remains above 450 km or when the resulting computed height of maximum density is lower than any portion of the raypath, the point of closest approach to the earth along the satellite connecting line is chosen as the reference point at which the profile is determined.

The electron density above the maximum is modeled in 6 layers, the lowest one being parabolic with a variable half-thickness, followed by 5 consecutive exponential layers with variable decay constants, see Figure 5. The heights at which the interfaces occur depend on the thickness of the layers. The points for computing additional density values along the leg from the reference point to the high satellite are determined to fall at the interfaces between the different layers, or at least close by, as they are encountered along the raypath. The numerical integration can later be performed over each segment-minimizing errors that can accumulate from integrating across layer

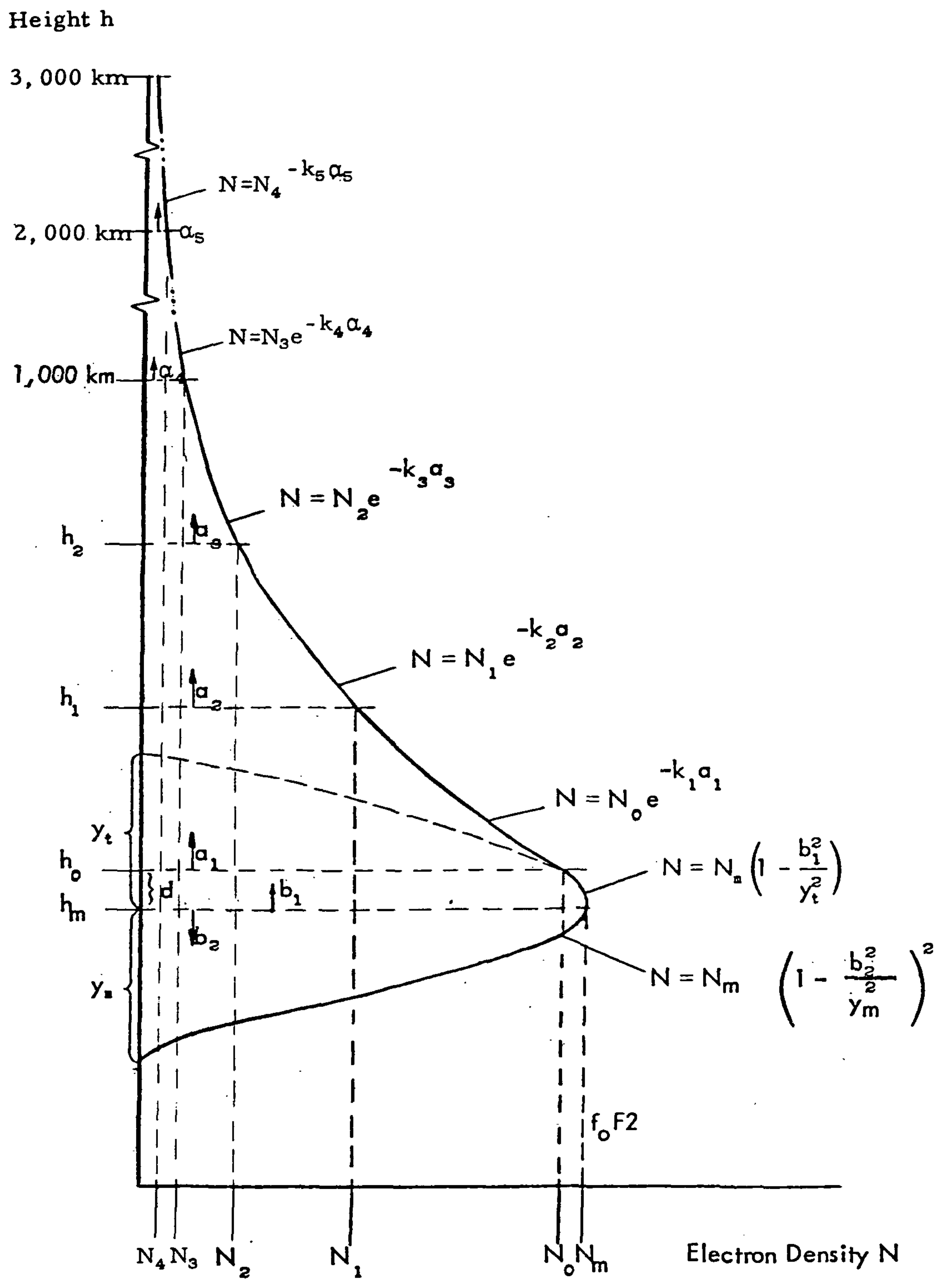

Fig 5. The Exponential Parabolic & Bi-parabolic Profile

boundaries. The intersections of the satellite raypath with the heights of the layers as computed from the profile at the reference point, determine the actual positions at which additional electron densities are evaluated using the ionospheric model.

When performing the precision tests, it was found necessary to insert an additional electron density computation half way between the reference point and the next higher point. It was also attempted to calculate the density values between every other exponential layer, but the results were not satisfactory. Altogether 8 points were chosen for computation along the high satellite leg at the following heights:

$h_1 = h_m$, h_m is the height of maximum density

$h_2 = h_m + \frac{d}{2}$, d is the distance above h_m where the parabolic and exponential layers meet

$h_3 = h_m + d$

$h_4 = h_m + d + \delta$, $\delta = (1012 \text{ km} - h_3)/3$

$h_5 = h_m + d + 2\delta$

$h_6 = 1000$ km

$h_7 = 2000$ km

$h_8 = 5000$ km

Whenever the low satellite is on the opposite side of the reference point to the high satellite, the ray may pass through very dense portions of the ionosphere, especially if the connection line remains in the maximum density region over an appreciable distance. For this reason it is important to evaluate the densities accurately along this segment. The ray may not cross the lower biparabolic model layer, but enter and exit from above, or it may not enter it at all. These geometrical considerations suggest that it is not sufficient to calculate the electron densities only at the layer interfaces as done along the high satellite leg. Instead, the model densities were reevaluated at regular intervals, starting at the low satellite and continuing in constant steps of earth central angle all the way to the reference point. To arrive at a proper step size, accuracy tests were performed using angular increments of 2, 3 and 4 degrees, and the 3 degree intervals in central angle were found to give satisfactory results.

In the specific cases where the low satellite leg passes through a segment of maximum electron density, it provided significant improvement in accuracy to insert an extra density computation exactly at the second height of maximum density. Hence, this feature was also included in the point selection technique.

The results from accuracy tests for various point selections along the low satellite leg are summarized in Table 1. Three cases of satellite configurations were chosen in March 1970 that were representative of highly refractive ionospheric situations. In these cases the ionosphere was dense as a function of solar activity, local time and geographic location, and the satellite connecting line crossed the height of maximum density twice and remained in the vicinity of the maximum over large distances. Electron densities along the path were computed from the ionospheric model at the selected 8 points between the reference profile and the high satellite, and at a varying number of points between the reference profile and the low satellite. The results shown are for point spacings at 2 and 3 degrees of earth central angle, including and excluding the calculations at the second maximum density. Between these points additional density values were inserted that were obtained from the spline interpolation, as described later. A numerical integration by Gaussian quadrature was performed over all density values yielding the results representative of the developed correction technique and tagged by "model value" in Table 1. These numbers were compared with the corrections marked as "exact value", which were computed by replacing the interpolated electron densities by the actual densities as determined from the ionospheric model. The difference between the two indicates the accuracy of the correction method.

The accuracy in range is much better than the required 2 cm value, it is generally less than 1 mm. However, the developed sophisticated

Table 1. Accuracy Test for Ionospheric Range and Range-Rate Corrections

Point Selection and Ion. Case Specification	Range Correction (m) Exact Value	Model Value	Accuracy	Range-Rate Correction (mm/sec) Exact Value	Model Value	Accuracy
1) 2° point spacing without 2nd max.						
case 1	.56147	.56214	.000663	2.13358	2.11934	.01424
case 2	1.93150	1.93188	.000378	.86152	.85283	.00869
case 3	.67561	.67688	.001270	1.66493	1.60436	.06056
2) 2° point spacing with 2nd max.						
case 1	.56147	.56176	.000290	2.13361	2.12531	.00830
case 2	1.93150	1.93199	.000491	.86158	.85577	.00582
case 3	.67561	.67566	.000045	1.66388	1.67416	-.01028
3) 3° point spacing without 2nd max.						
case 1	.56148	.56213	.000644	2.13208	2.12065	.01142
case 2	1.93151	1.93214	.000626	.86163	.84967	.01197
case 3	.67560	.67621	.000612	1.66622	1.66783	-.00160
4) 3° point spacing with 2nd max.						
case 1	.56148	.56212	.000638	2.13208	2.12060	.01147
case 2	1.93151	1.93215	.000637	.86147	.84970	.01177
case 3	.67560	.67624	.000633	1.66622	1.66745	-.00123

Desired accuracy in range .02 m, and in range-rate .03 mm/sec technique is necessary for the range-rate accuracy to be better than .03 mm/sec. In Table 1 between 1) and 2), case 3, great improvement is obtained by adding a point at the second maximum. It is not as apparent under 3) and 4), because the 3 degree spacing happened to locate a point already close to the maximum, while for 2 degree spacing the maximum just fell between two points. The range-rate corrections for the selected technique in these extreme situations show accuracies of .01 mm/sec and better.

Curve Fitting for Interpolation

The cubic spline interpolation was chosen for fitting the electron density values as a function of distance, defining the density values at intermediate points. Polynomial fits that had been attempted did not yield satisfactory results. The cubic spline interpolation accepts any number of points at irregular intervals, and requires the slopes at both end points. From this information the spline computes the slope and radius of curvature as first and second derivatives at all intermediate points, and fits a third or lower order curve exactly through any set of four points.

When the spline interpolation was applied, a number of considerations were found to have a significant influence on obtaining good results, and the correction technique was adjusted accordingly. While the interpolation is very good, extrapolating yields poor results. Points are accepted at uneven spacing, but if the intervals are not of the same order of magnitude the fit might show instabilities. Good slope computations at the end points are quite significant.

At first the slope for the spline on the high satellite end was determined at a height of 2000 km. Since the integration was to be performed out to a height of 5000 km, additional points past 2000 km were extrapolated resulting in poor integration results. The technique was then modified to compute the end slope at 5000 km so that only interpolation was required, and the problem was thus eliminated.

By inserting a second maximum into the point selection and by spacing off 3 degree steps from the low satellite to the reference point, it could occur by chance that either at the second maximum, at the reference point or at the low satellite, the interval between points would be several orders of magnitude smaller than the normal spacing between points. Since it had been found in some cases that this condition might result in an instability in the curve fitting leading to very large errors, logical tests for these cases were inserted to eliminate one of the close points when such a condition occurred.

The slopes at the end points are computed by differencing two adjacent electron density values and dividing by the distance, thus assuming linear curve segments at the ends. The slopes had been computed over a distance of 50 km which was changed to 1 km. The 1 km distance gave a more accurate slope under the linear assumption, and this distance was still large enough to ensure the numerical stability in the model densities. Problems still persisted if the end slope was computed in a region of very high electron density where the ionospheric gradient was large and changing. If the very sudden variations that can occur in the densities happened between the last two points, they induced instabilities in the curve fit. An additional logical test was included to eliminate end slope computations in the vicinity of the maximum electron density by moving the 2 end points a distance of 100 km away from the height of the maximum. The curve fit across the densest portion was then stable and resulted in accurate values.

Numerical Integration

The total integration was carried out from the low satellite toward the high satellite out to a height of 5000 km. A considerable electron density can still be encountered between 1000 and 5000 km especially along slanted paths, but above 5000 km along vertical paths the density accumulated generally amounts to much less than 1% and under adverse conditions to at most 6 % of the total ground to satellite electron density. The corresponding test results obtained from the ionospheric model are given in Table 2.

The electron densities as a function of distance along the raypath from the low to the high satellite were integrated numerically by Gaussian quadrature. The intervals between the selected points at which the densities were obtained from the ionospheric model represent the exponential profile layers and segments of the parabolic and biparabolic layers. Each interval of the profile was integrated separately with a varying number of points to achieve maximum accuracy. The distribution of the points in the interval is symmetrical about the centerpoint as determined by the Gaussian method, and the densities at these points are evaluated using the cubic spline interpolation. Three points are positioned in each of the upper exponential layers, and five points are spaced over each of the lower profile segments. Tests were performed by doubling the number of points in each interval for use in the numerical integration, but no significant improvement was obtained over the previous results. The selection of three and five points was found satisfactory in terms of accuracy achieved.

The integrated electron densities between the low and high satellites were converted to refraction corrections for the range and range-rate measurements along the communication link by use of equations (3-2) and (3-3).

Table 2. Distribution of Electron Density with Height

Solar Activity /Date	UT (hours)	Magnetic Latitude of Location (degrees)	Percentage of Ground-to-Satellite Electron Density Located Above 1000 km	3000 km	5000 km
High 16 Mar 67	14	10	9.56	3.33	1.41
	11	39	12.30	1.85	0.34
	12	80	14.12	0.79	0.07
Med. High 20 June 71	18	10	23.54	10.41	5.21
	18	39	13.39	2.39	0.52
	18	80	13.13	0.79	0.04
Low 10 Dec 65	6	10	23.26	11.88	6.36
	6	39	22.20	6.65	2.18
	6	80	8.26	0.80	0.12

5.0 DATA SELECTION AND REDUCTION

The GRAVSAT and GEOPAUSE satellites were assumed in circular, coplanar polar orbits with the following parameters:

Parameters	GRAVSAT	GEOPAUSE
semi-major axis a (km)	6,678	29,431
eccentricity e	0	0
inclination i (deg)	90	90
argument of perigee ω (deg)	180	180
orbit period T (hours)	1.5	14.0

GEOPAUSE, when visible, was tracked from the six ground stations: Canberra, Johannesburg, Santiago, Guam, Madrid and Rosman. The S-band frequencies used along the various legs of the communication link were:

ground to geopause -	2.0 GHz
geopause to gravsat -	13.0 GHz
gravsat to geopause -	14.0 GHz
geopause to ground -	2.2 GHz

These frequencies, combined to average values of 2.093 GHz for the ground link and 13.472 GHz for the satellite link with the aid of equation (3-3), were used to compute the one-way ionospheric range and range-rate corrections.

The two satellite orbits were generated at 1 minute intervals for the evaluation of refraction effects. Since the range-rate corrections were obtained by differencing range corrections over 10 second increments, additional positions were produced at 10 seconds past each minute mark. The start points for both orbits were chosen such that the satellites just became visible to each other over the horizon, and that the connecting line passed through the equational anomaly, a very dense portion of the ionosphere exhibiting extremely high gradients. The date of 23 December 1969 was selected, which was during a period of high solar activity at the peak of the last sunspot cycle. The local time was specified as 16 hours for the start point. Everything was geared toward producing very severe ionospheric refraction conditions, in order to examine some extreme situations, as well as the more typical ones along the satellite-to-satellite link. The coordinates for the initial positions of the satellites are presented in the table below for the 6 cases used in the data reduction. For each case data was generated over 2 complete revolutions of the low satellite.

Case	Universal Time (hours)	GRAVSAT Latitude	GRAVSAT Longitude	GEOPAUSE Latitude	GEOPAUSE Longitude (degrees)
1	9	40	105	54.746	105
2	9	45	105	49.746	105
3	9	50	105	44.746	105
4	11	40	75	54.746	75
5	11	45	75	49.746	75
6	11	50	75	44.746	75

For the selected dates and start times world maps of ionospheric contours of the critical frequencies $f_o F2$ and the heights of maximum electron density h_m were drawn, as presented in Figures 6a, b and 7a, b. The satellite orbits are superimposed, although it has to be noted that the ionospheric contours are drawn for the start times and would change over the 3 hour tracking period investigated. The raypath in Figures 6a, b from any of the low to the high satellite positions can be visualized penetrating the high gradient portion of the ionosphere in the equatorial anomaly when the altitude of the ray is of the order of h_m. In Figures 7a, b the variations in the height of maximum electron density are shown. It was anticipated that the satellite connection line would increase in altitude over the segment where h_m exhibits large positive gradients. In this manner situations were constructed where for short periods of time the raypath would follow along the maximum height h_m, encountering maximum electron density conditions over hundreds of kilometers.

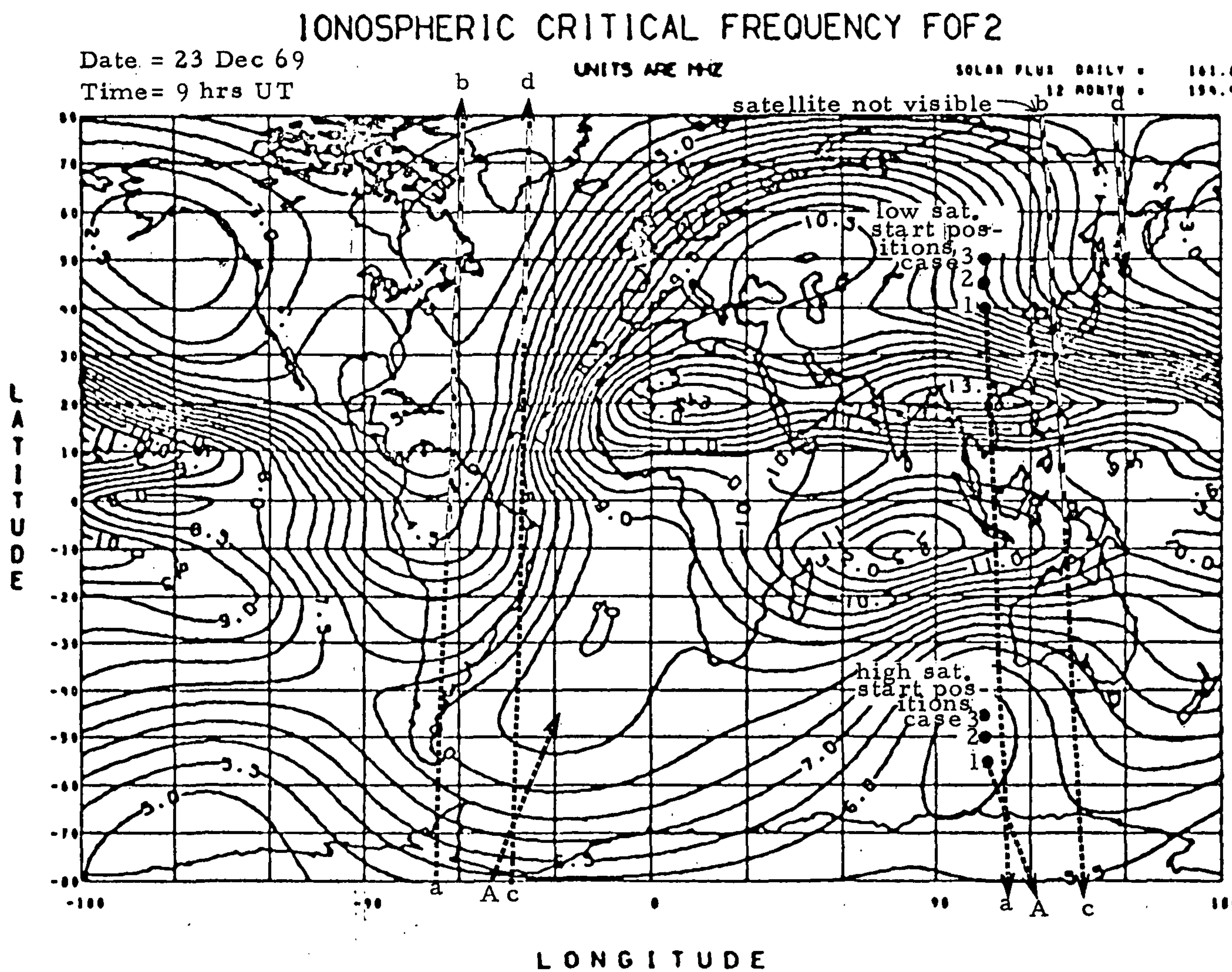

Figure 6a. Worldmap of Critical Frequencies with Satellite Orbits

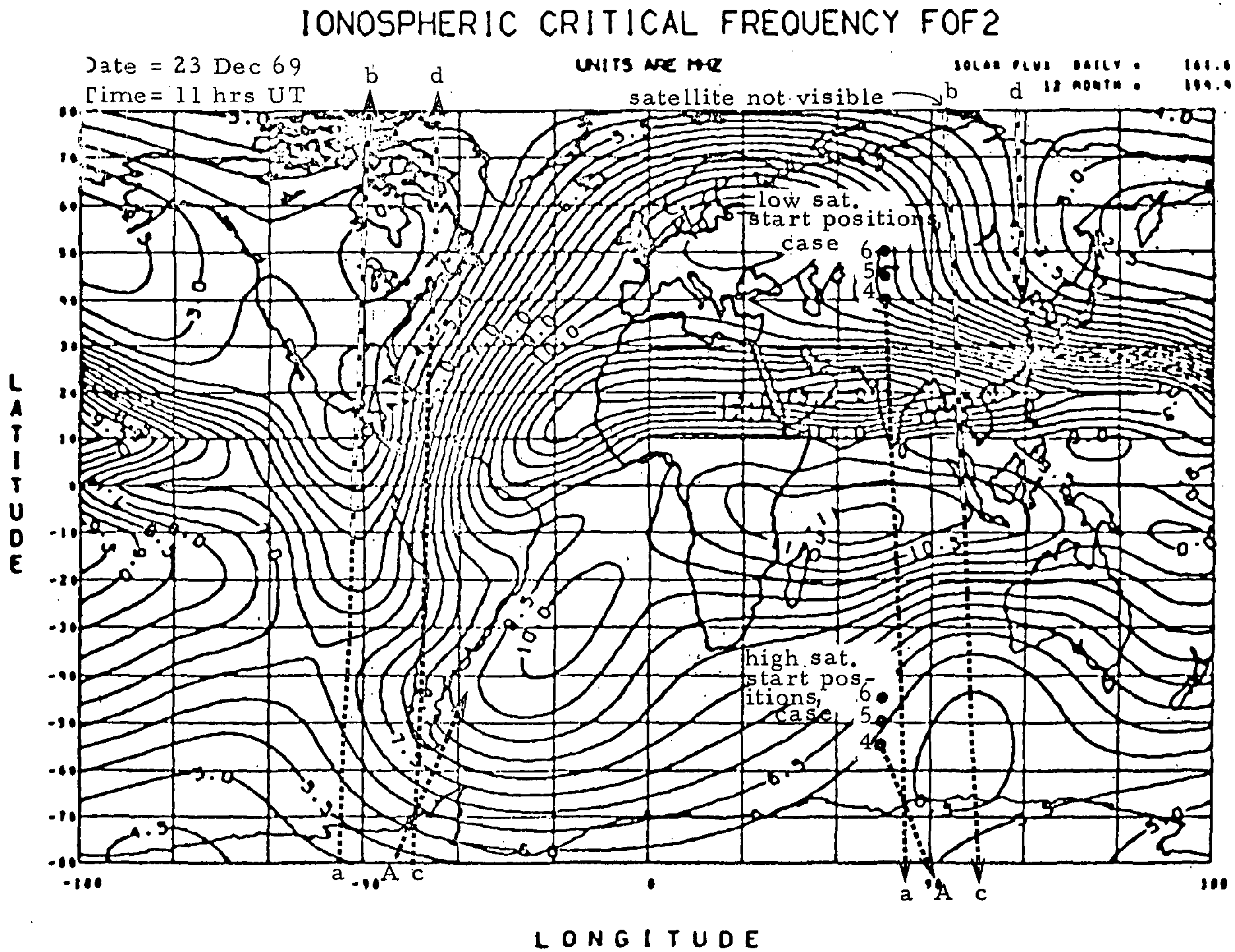

Figure 6b. Worldmap of Critical Frequencies with Satellite Orbits

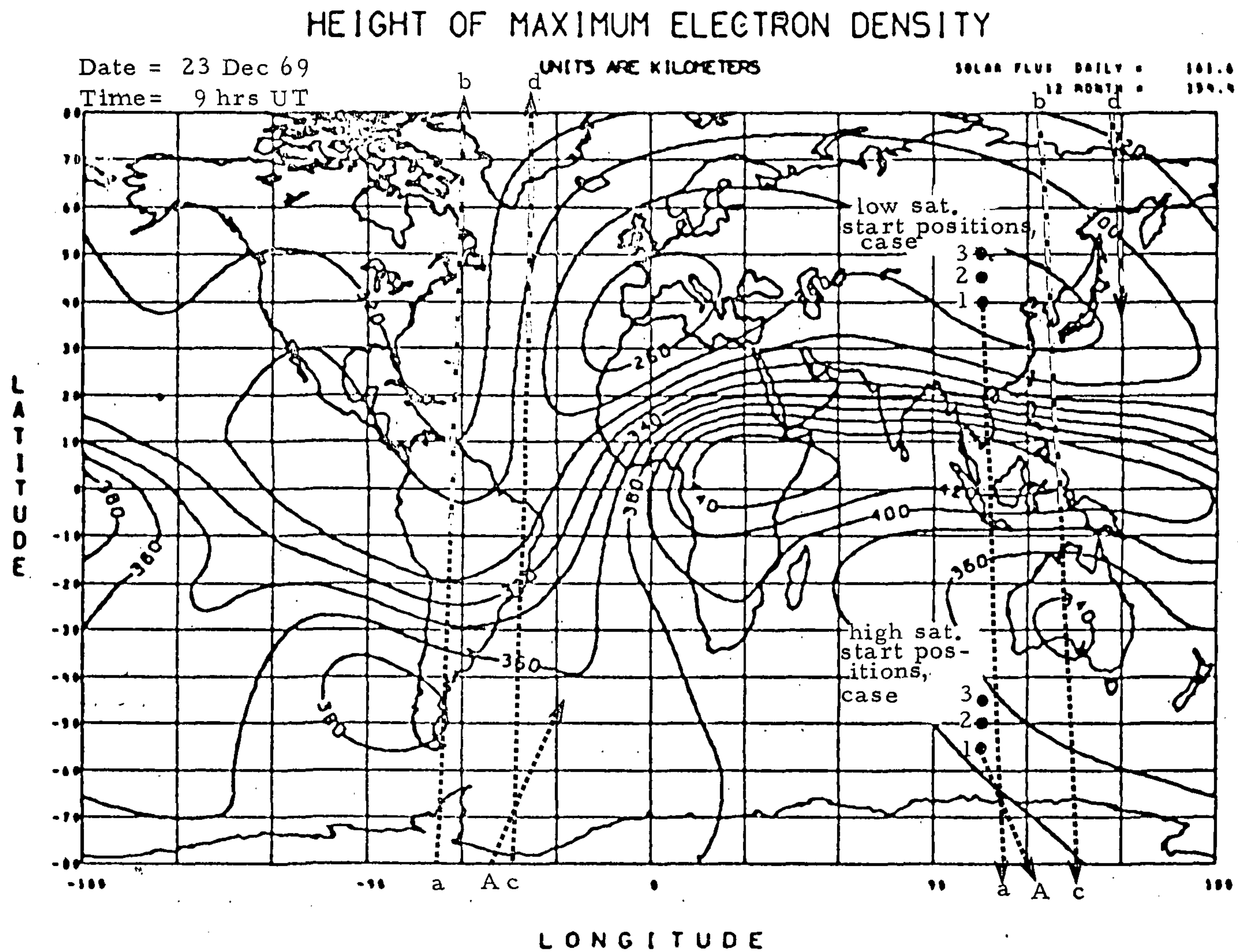

Figure 7a. Worldmap of h_m with Satellite Orbits

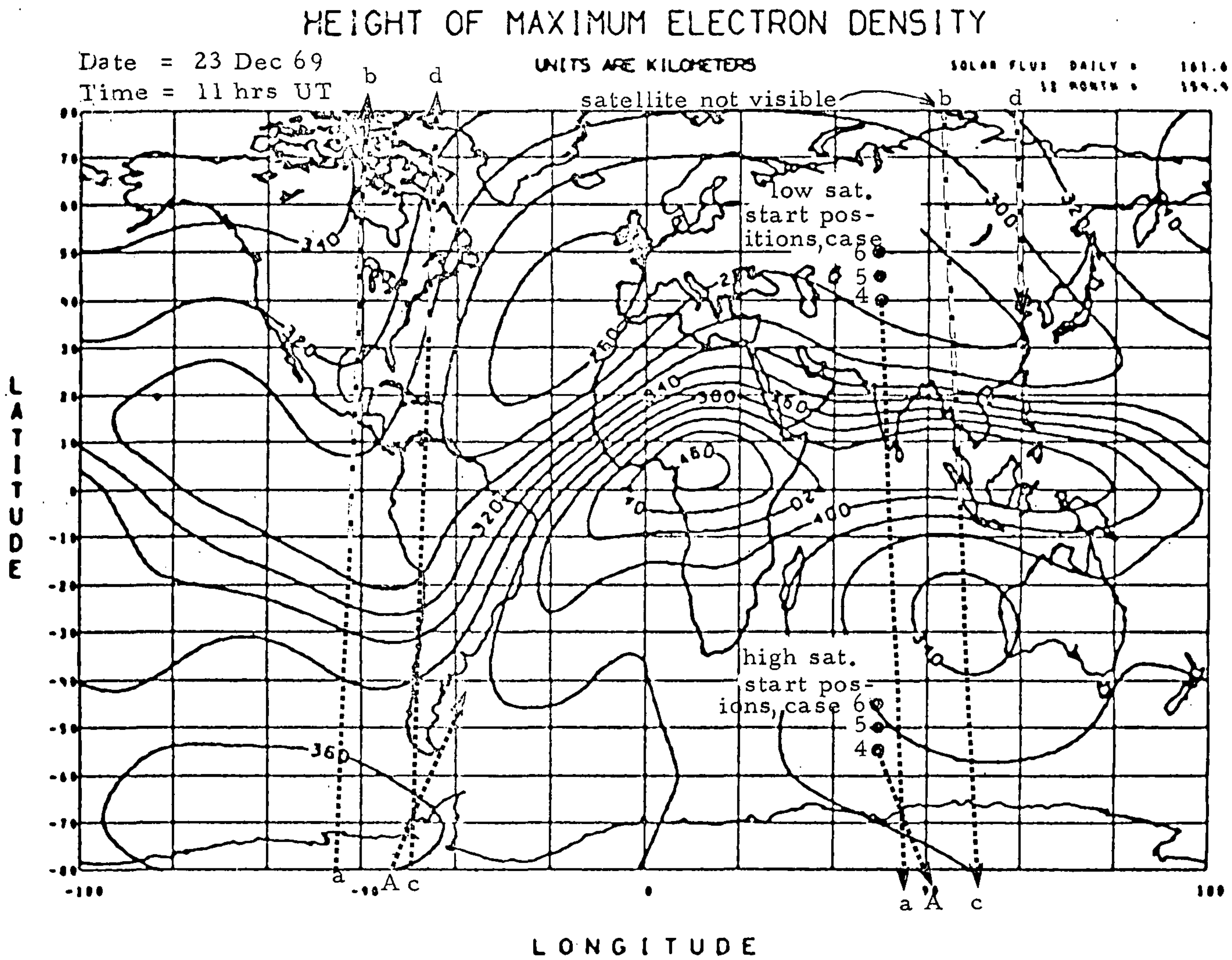

Figure 7b. Worldmap of h_m with Satellite Orbits

Refraction corrections to range and range-rate were computed once per minute over each 3 hour period. The results for the ionospheric corrections along the satellite-to-satellite link were plotted against time in Figures 9a-l for all 6 cases. Tropospheric corrections for the satellite link are included in the same graphs. The satellite rises so quickly over the horizon, that tropospheric effects are experienced only at the first point of the pass and already a minute later the raypath remains completely above the troposphere. Typical tropospheric errors for any type of raypath geometry are shown in Figures 2 and 3. Figures 10a-f are plots of the ionospheric corrections along the ground link for cases 4-6. Since GEOPAUSE remains south of -54 degrees in the southern hemisphere during the two orbits of GRAVSAT, it is visible only from the tracking stations Canberra, Johannesburg and Santiago. The tropospheric refraction corrections along the ground link for cases 4-6 are shown in Figures 11a-f. Figure 8 summarizes all of the refraction corrections for case 5.

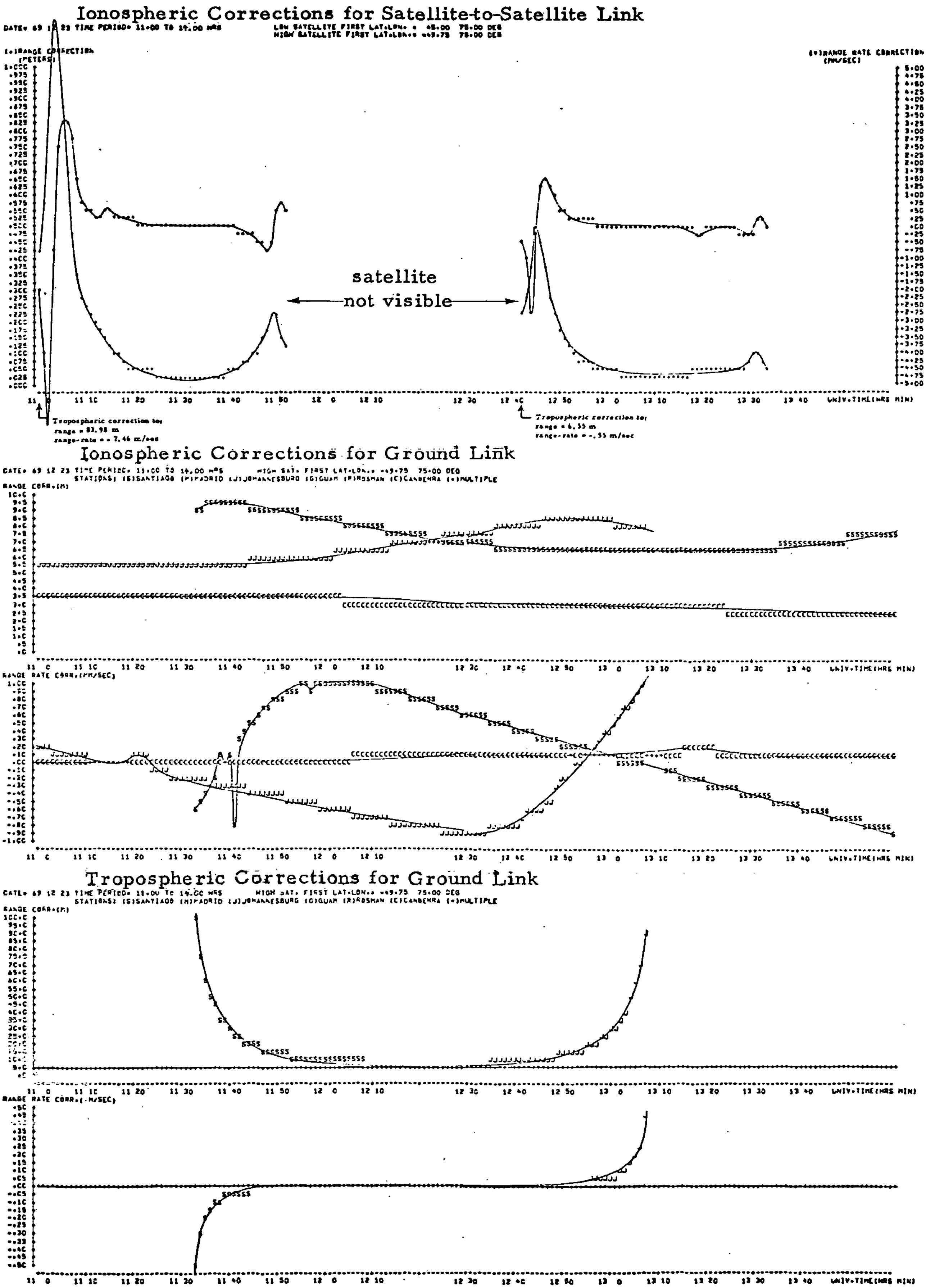

Figure 8. Trop. and Ion. Corrections to Range and Range-Rate along Ground and Sat. Links for Case 5

6.0 SUMMARY OF RESULTS

For the satellite-to-satellite tracking configuration accuracies of the order of .02 meters in range and of .03 mm/sec in range-rate were specified. The consistency in the technique of computing the refraction corrections exceeded these requirements, and accuracies of .0006 m in range and .011 mm/sec in range-rate or better were achieved, see Table 1. The Bent Ionospheric Model, on which the technique was based, estimates an average 75 percent of the refraction effects in its prediction mode in which it was used, and this accuracy can be increased to 90 percent when updating with actual ionospheric observations.

The refraction results for 6 selected orbits, each lasting over two revolutions of the low satellite are listed in Figures 8-11. These values represent the one-way corrections along the different communication links. The ionospheric computations were based on an average of the uplink and downlink frequencies for each leg, and the specific frequencies are given in Section 5.0. This allows the total refraction effects for the closed communication loop to be determined by simply doubling the corrections for each link and summing. It was chosen to represent tropospheric and ionospheric effects along ground and satellite links separately so that the results could be examined for the independent variation of each contribution and that the problem areas could be isolated.

The size of the ionospheric range and range-rate corrections is directly dependent on the square of the critical frequency. For the points of the presented cases that exhibited the most severe refraction effects, the frequencies encountered at the segments of maximum electron density along the satellite-to-satellite link were between 8 and 14 MHz. A median f_oF2 value under extreme refraction conditions would be about 16 MHz, and considering the square relationship, would result in much larger range and range-rate corrections than were obtained for the test cases. This is illustrated in Table 3, and it should be kept in mind when examining Figures 8 and 9a-l.

Table 3. Summary of Maximum Refraction Corrections

Communication Link	Refraction Type	Maximum refraction corrections obtained for selected orbits		Corrections possible under extreme refraction conditions based on a median f_oF2 value of 16 MHz	
		ΔR (m)	$\lvert\Delta\dot{R}\rvert$ (mm/sec)	ΔR (m)	$\lvert\Delta\dot{R}\rvert$ (mm/sec)
Satellite Link	Ionospheric				
	at 13.472 GHz	1.17	9.21	2.64 *	17.31
	normalized to 1 GHz	212.35	1671.57	479.15 *	3142.12
	Tropospheric	84.24	7495.00	260.00 o	23000.00 o
Ground Link	Ionospheric				
	at 2.093 GHz	9.48	1.01	24.27	3.19
	normalized to 1 GHz	41.53	4.42	106.32	13.97
	Tropospheric	101.10	500.00	130.00	500.00

* based on test case 2 where ΔR = 1.93 m (Table 1)

o ray passing just above earth's surface in equatonial region (Figures 2, 3);
these corrections apply only to the first 20 sec of each satellite pass, all other corrections = 0.

For the defined tracking system the tropospheric refraction effects are mostly dominant over the ionospheric ones. Along the ground link the tropospheric range errors were between 5 and 100 m and range-rate errors were between 0 and $\pm$ .5 m/sec. Along the satellite link the range errors were of the same order as along the ground link, but significantly larger range-rate errors of up to -7.5 m/sec existed. This was because the ground stations were observing the slow moving GEOPAUSE, while GEOPAUSE was tracking the fast orbiting GRAVSAT. For the latter geometry the ranges and associated errors are changing much more rapidly giving rise to much larger range-rate errors. The troposphere effects the satellite-to-satellite tracking only within the first and last 30 seconds of each pass, when GRAVSAT is just about to appear or disappear under the horizon from the view of GEOPAUSE. For other satellite configurations the connecting raypath remains completely above the height of the troposphere. This circumstance greatly reduces the problem of tropospheric errors along the satellite link, and for practical purposes it might be considered to completely ignore any tropospheric refraction, and to deal with the rare points that are effected by editing them out of any data reduction process.

Ionospheric refraction along the ground link was found to yield errors between 2.5 and 9.5 m in range and 0 to $\pm$ 1mm/sec in range-rate. The large errors occurred when GEOPAUSE just became visible from the tracking stations. The satellite positions relative to the ground stations during the tracking period under consideration were at elevation angles of less than 1 degree to 35 degrees.

Because the communication frequencies used along the satellite leg were 6.4 times as high as those used for the ground link, the range errors accumulated along the satellite link were between 0 and 1.2 m, and were much smaller than the errors along the ground leg, even though the number of electrons encountered along the path was much greater. The maximum refraction errors due to tropospheric and ionospheric effects are summarized in Table 3, and a column is included that normalizes the ionospheric corrections to a frequency of 1 GHz. From this tabulation it is apparent that the total electron density encountered along the raypath between the satellites is 5 times as high as along the ground leg, considering the extreme cases in both instances. The range-rate corrections along the satellite link were between +4 and -9 mm/sec, and, as in the tropospheric case, they were much larger than the corrections for the ground link because of the satellite geometry and angular velocity.

The ionospheric critical frequencies encountered in the calculations of the selected tests were noticeably smaller than a median value of 16 MHz for extreme refraction conditions. To indicate maximum possible errors, an extra column was added to Table 3 showing the errors that were obtained when the critical frequencies involved in the test cases were projected out to 16 MHz. Even though the corrections along the ground and the satellite links are independent of one another, certain maximum error conditions could by chance be obtained simultaneously at certain times, amounting to extremely severe total refraction errors in the observation data.

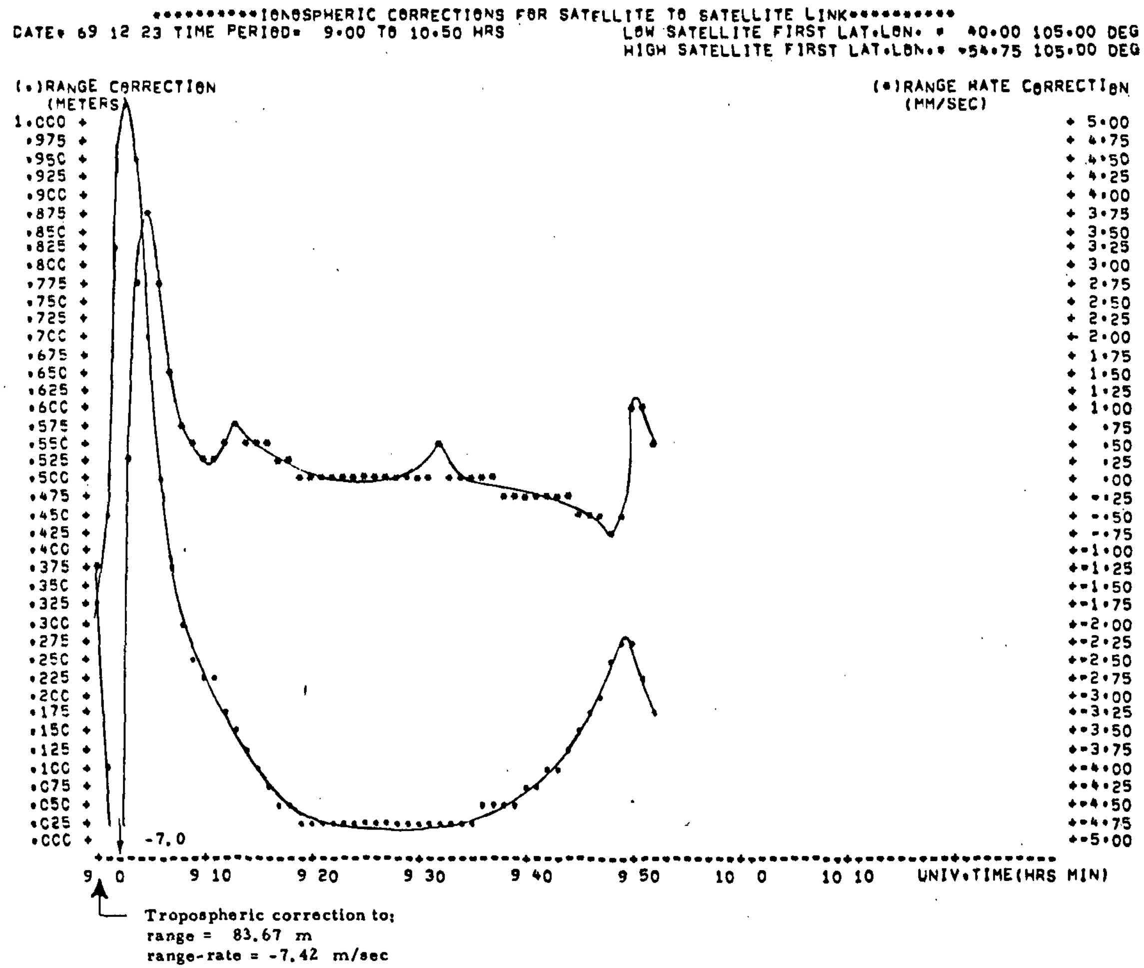

**********IONOSPHERIC CORRECTIONS FOR SATELLITE TO SATELLITE LINK**********
DATE* 69 12 23 TIME PERIOD* 9.00 TO 10.50 HRS
LOW SATELLITE FIRST LAT.LON. * 40.00 105.00 DEG
HIGH SATELLITE FIRST LAT.LON.* *54.75 105.00 DEG
(.)RANGE CORRECTION (METERS)
(*)RANGE RATE CORRECTION (MM/SEC)
1.000 .975 .950 .925 .900 .875 .850 .825 .800 .775 .750 .725 .700 .675 .650 .625 .600 .575 .550 .525 .500 .475 .450 .425 .400 .375 .350 .325 .300 .275 .250 .225 .200 .175 .150 .125 .100 .075 .050 .025 .000
5.00 4.75 4.50 4.25 4.00 3.75 3.50 3.25 3.00 2.75 2.50 2.25 2.00 1.75 1.50 1.25 1.00 .75 .50 .25 .00 -.25 -.50 -.75 -1.00 -1.25 -1.50 -1.75 -2.00 -2.25 -2.50 -2.75 -3.00 -3.25 -3.50 -3.75 -4.00 -4.25 -4.50 -4.75 -5.00
-7.0
9 0 9 10 9 20 9 30 9 40 9 50 10 0 10 10 UNIV.TIME(HRS MIN)
Tropospheric correction to:
range = 83.67 m
range-rate = -7.42 m/sec

Figure 9a.

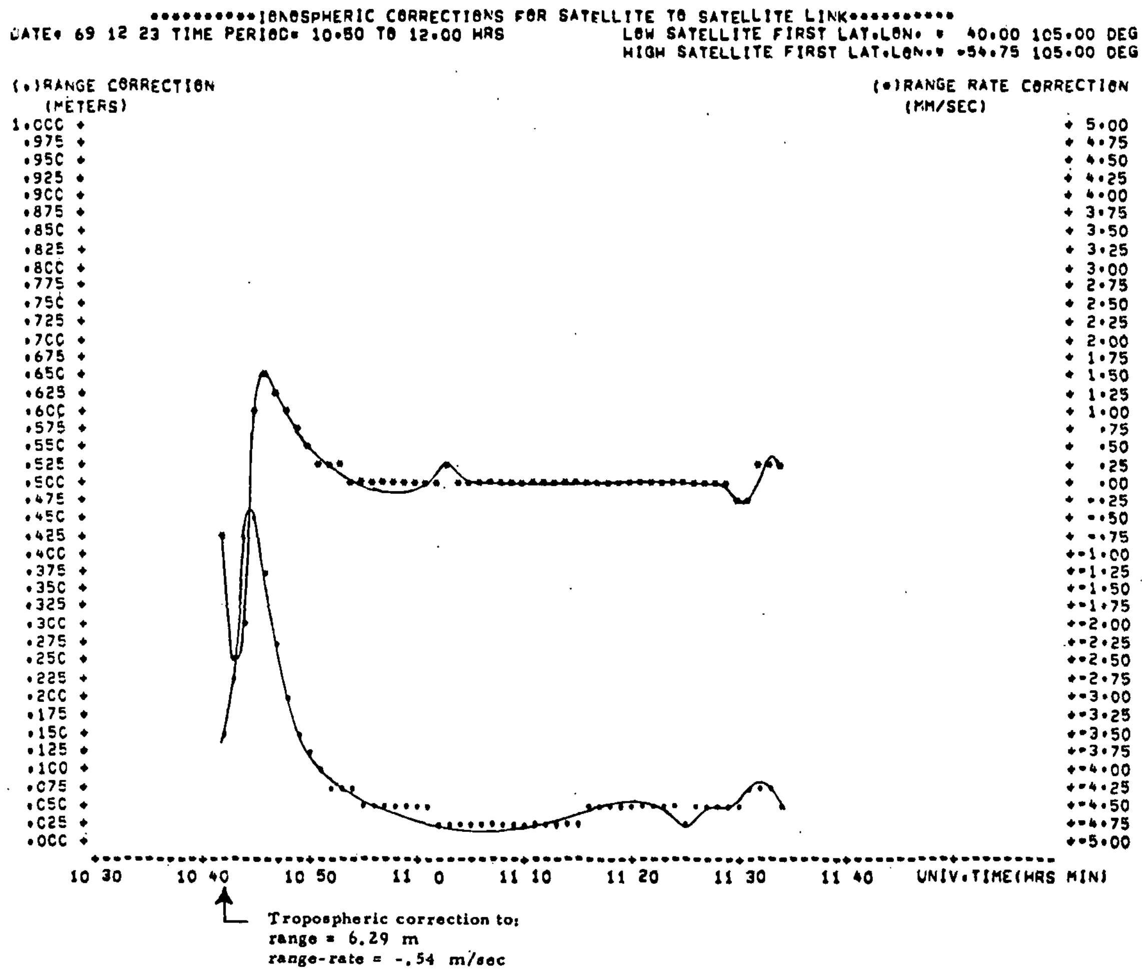
**********IONOSPHERIC CORRECTIONS FOR SATELLITE TO SATELLITE LINK**********
DATE, 69 12 23 TIME PERIOD, 10.50 TO 12.00 HRS
LOW SATELLITE FIRST LAT.LON. = 40.00 105.00 DEG
HIGH SATELLITE FIRST LAT.LON.= -54.75 105.00 DEG
(.)RANGE CORRECTION
(METERS)
(*)RANGE RATE CORRECTION
(MM/SEC)
UNIV.TIME(HRS MIN)
Tropospheric correction to:
range = 6.29 m
range-rate = -.54 m/sec

Figure 9b.

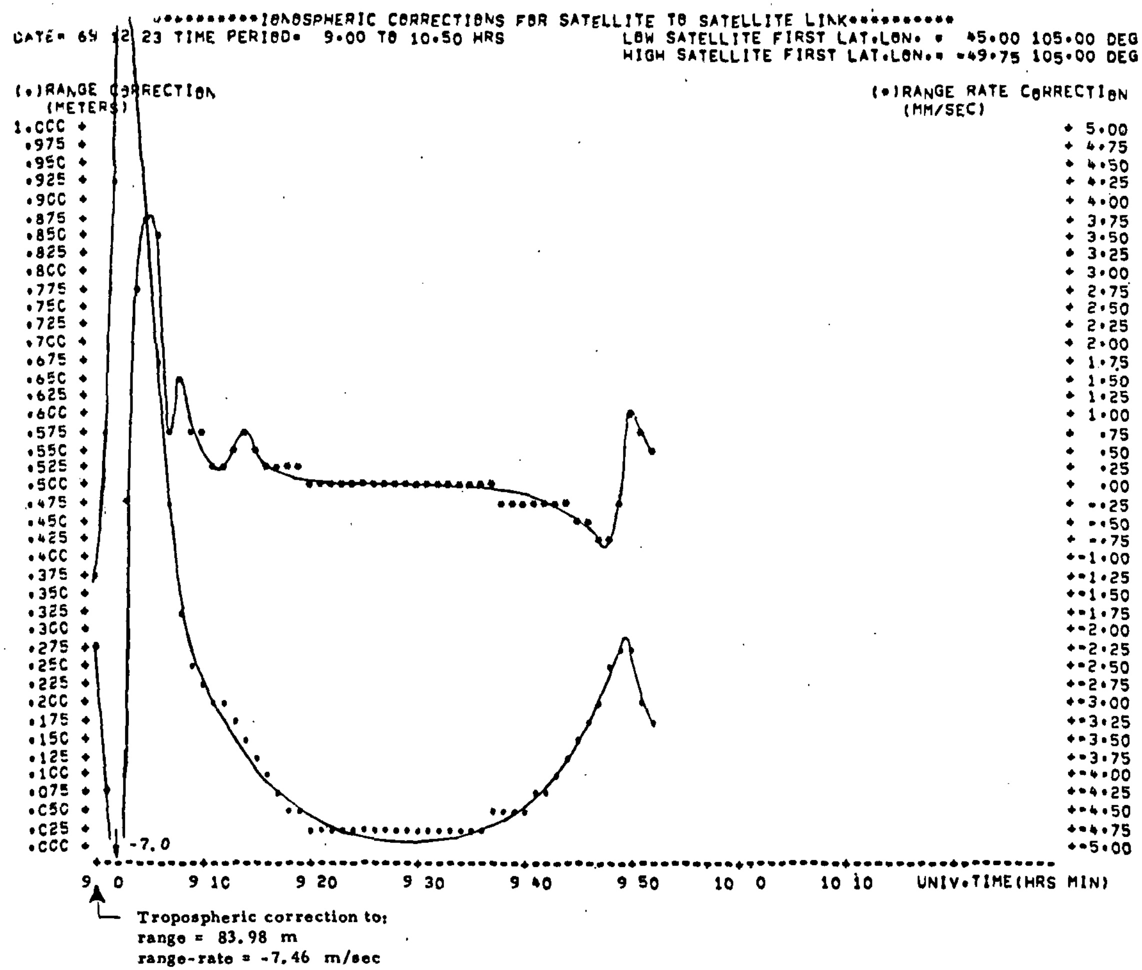
IONOSPHERIC CORRECTIONS FOR SATELLITE TO SATELLITE LINK
DATE= 69 12 23 TIME PERIOD= 9.00 TO 10.50 HRS
LOW SATELLITE FIRST LAT.LON. = 45.00 105.00 DEG
HIGH SATELLITE FIRST LAT.LON. = 49.75 105.00 DEG
(.)RANGE CORRECTION (METERS)
(*)RANGE RATE CORRECTION (MM/SEC)
-7.0
9 0
9 10
9 20
9 30
9 40
9 50
10 0
10 10
UNIV.TIME(HRS MIN)
Tropospheric correction to:
range = 83.98 m
range-rate = -7.46 m/sec

Figure 9c.

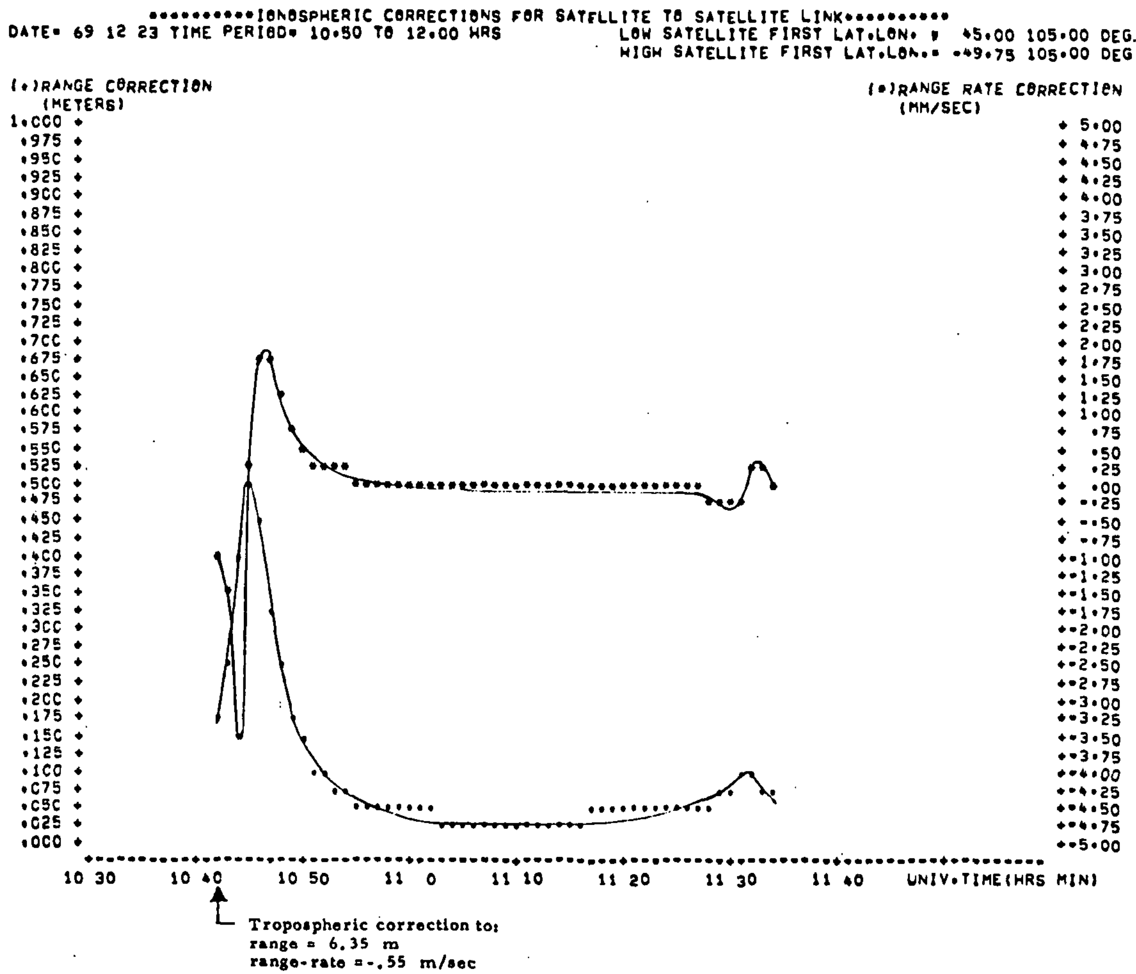
IONOSPHERIC CORRECTIONS FOR SATELLITE TO SATELLITE LINK
DATE= 69 12 23 TIME PERIOD= 10.50 TO 12.00 HRS
LOW SATELLITE FIRST LAT.LON. = 45.00 105.00 DEG.
HIGH SATELLITE FIRST LAT.LON. = -49.75 105.00 DEG
(+)RANGE CORRECTION
(METERS)
(*)RANGE RATE CORRECTION
(MM/SEC)
1.000
.975
.950
.925
.900
.875
.850
.825
.800
.775
.750
.725
.700
.675
.650
.625
.600
.575
.550
.525
.500
.475
.450
.425
.400
.375
.350
.325
.300
.275
.250
.225
.200
.175
.150
.125
.100
.075
.050
.025
.000
5.00
4.75
4.50
4.25
4.00
3.75
3.50
3.25
3.00
2.75
2.50
2.25
2.00
1.75
1.50
1.25
1.00
.75
.50
.25
.00
-.25
-.50
-.75
-1.00
-1.25
-1.50
-1.75
-2.00
-2.25
-2.50
-2.75
-3.00
-3.25
-3.50
-3.75
-4.00
-4.25
-4.50
-4.75
-5.00
10 30
10 40
10 50
11 0
11 10
11 20
11 30
11 40
UNIV.TIME(HRS MIN)
Tropospheric correction to:
range = 6.35 m
range-rate = -.55 m/sec

Figure 9d.

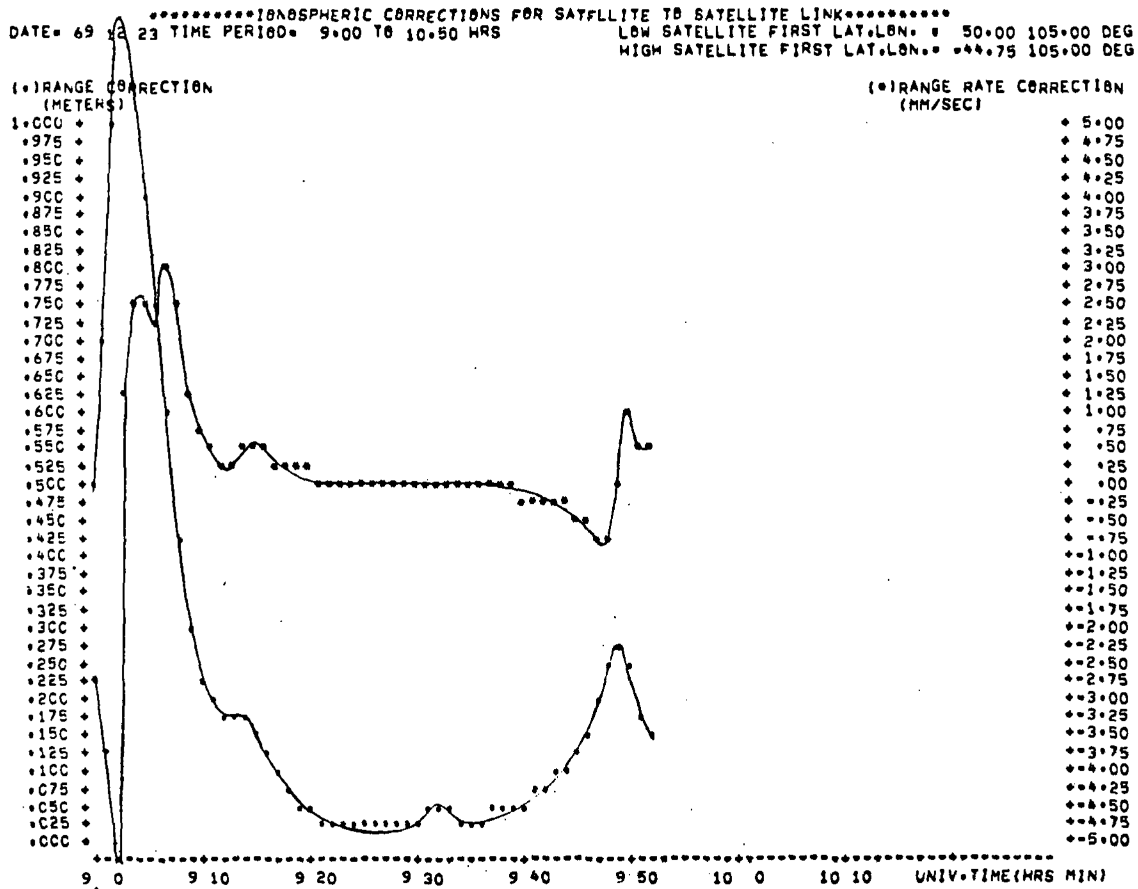

Tropospheric correction to:
range = 84.24 m
range-rate = -7.49 m/sec

Figure 9e.

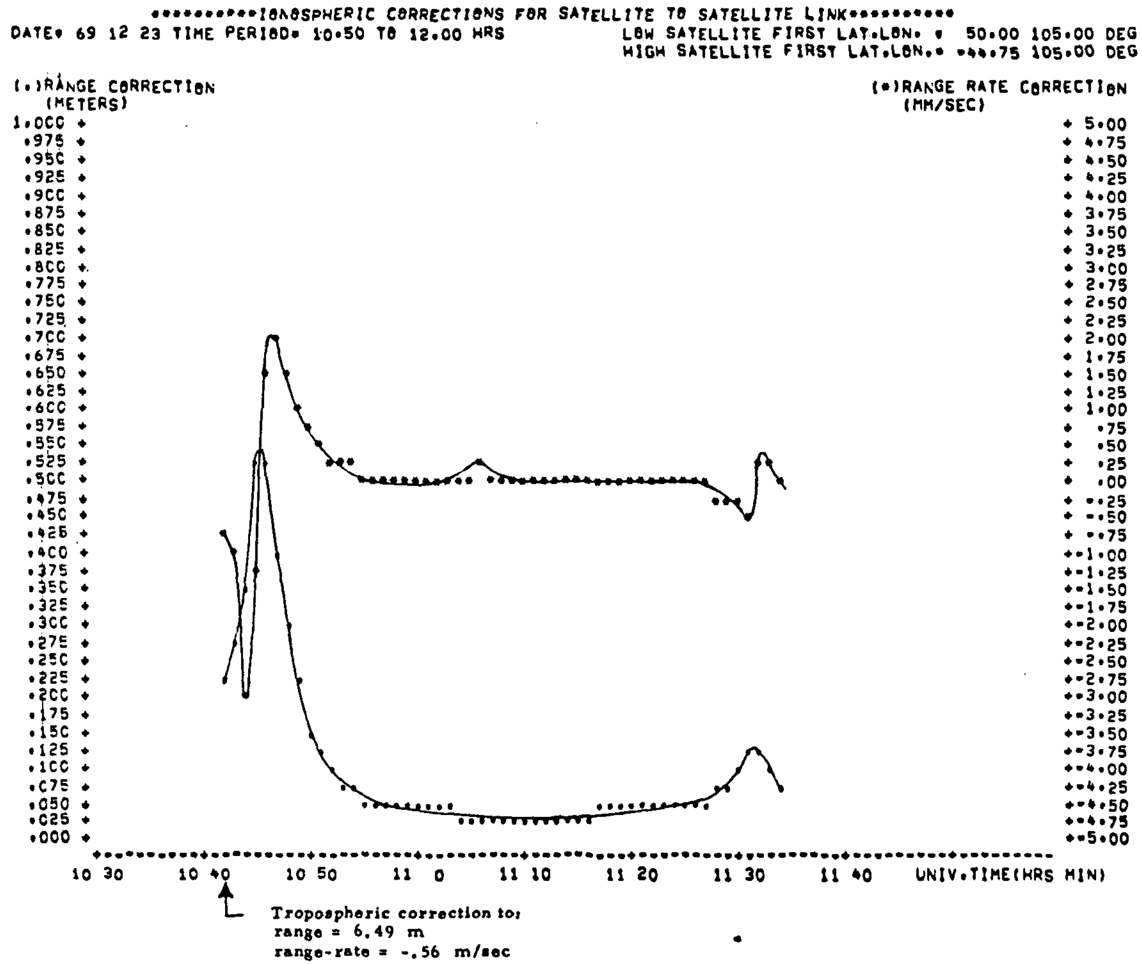
**********IONOSPHERIC CORRECTIONS FOR SATELLITE TO SATELLITE LINK**********
DATE, 69 12 23 TIME PERIOD, 10.50 TO 12.00 HRS
LOW SATELLITE FIRST LAT.LON. , 50.00 105.00 DEG
HIGH SATELLITE FIRST LAT.LON., -44.75 105.00 DEG
(.)RANGE CORRECTION (METERS)
(*)RANGE RATE CORRECTION (MM/SEC)
1.000 .975 .950 .925 .900 .875 .850 .825 .800 .775 .750 .725 .700 .675 .650 .625 .600 .575 .550 .525 .500 .475 .450 .425 .400 .375 .350 .325 .300 .275 .250 .225 .200 .175 .150 .125 .100 .075 .050 .025 .000
5.00 4.75 4.50 4.25 4.00 3.75 3.50 3.25 3.00 2.75 2.50 2.25 2.00 1.75 1.50 1.25 1.00 .75 .50 .25 .00 -.25 -.50 -.75 -1.00 -1.25 -1.50 -1.75 -2.00 -2.25 -2.50 -2.75 -3.00 -3.25 -3.50 -3.75 -4.00 -4.25 -4.50 -4.75 -5.00
10 30 10 40 10 50 11 0 11 10 11 20 11 30 11 40 UNIV.TIME(HRS MIN)
Tropospheric correction to:
range = 6.49 m
range-rate = -.56 m/sec

Figure 9f.

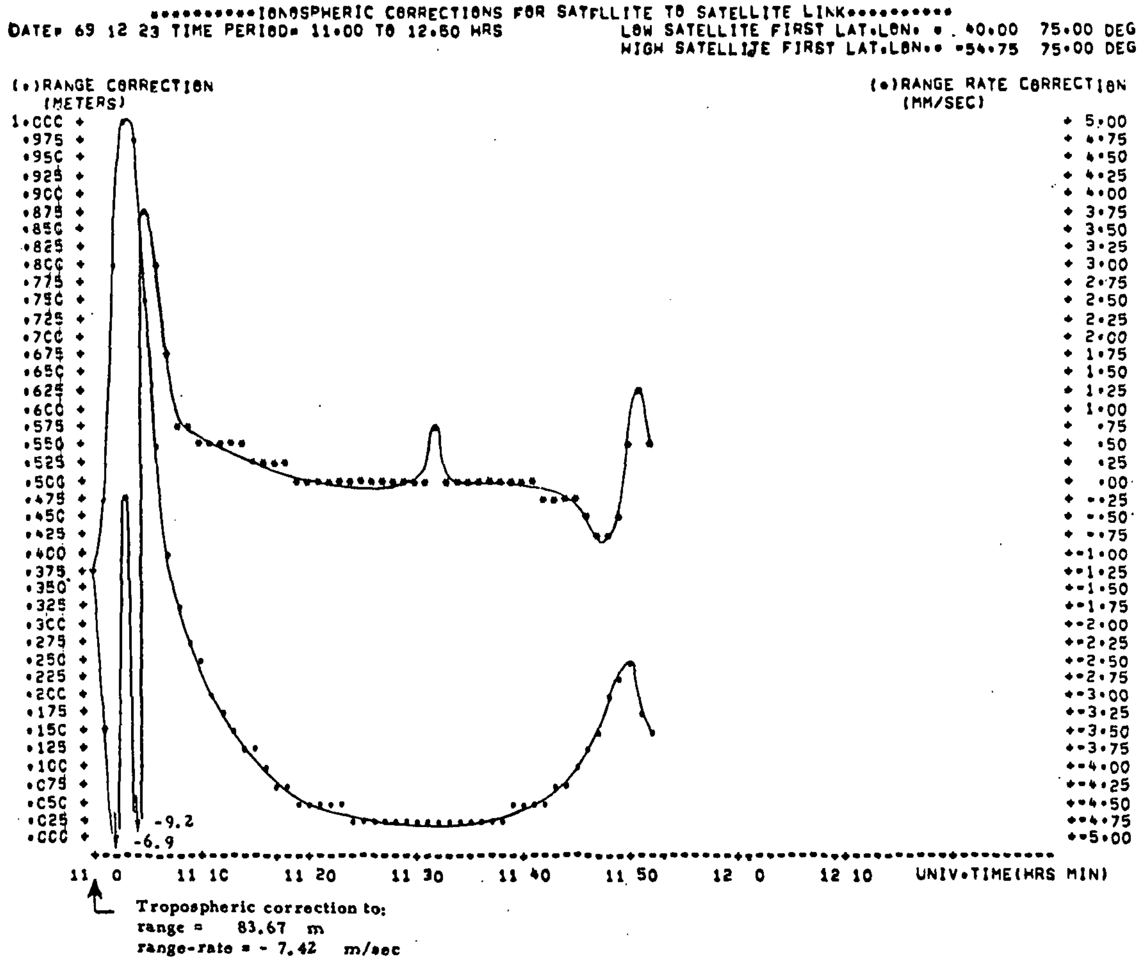
IONOSPHERIC CORRECTIONS FOR SATELLITE TO SATELLITE LINK
DATE= 69 12 23 TIME PERIOD= 11.00 TO 12.50 HRS
LOW SATELLITE FIRST LAT.LON. = 40.00 75.00 DEG
HIGH SATELLITE FIRST LAT.LON. = -54.75 75.00 DEG
(+)RANGE CORRECTION (METERS)
(•)RANGE RATE CORRECTION (MM/SEC)
-9.2
-6.9
11 0
11 10
11 20
11 30
11 40
11 50
12 0
12 10
UNIV.TIME(HRS MIN)
Tropospheric correction to:
range = 83.67 m
range-rate = - 7.42 m/sec

Figure 9g.

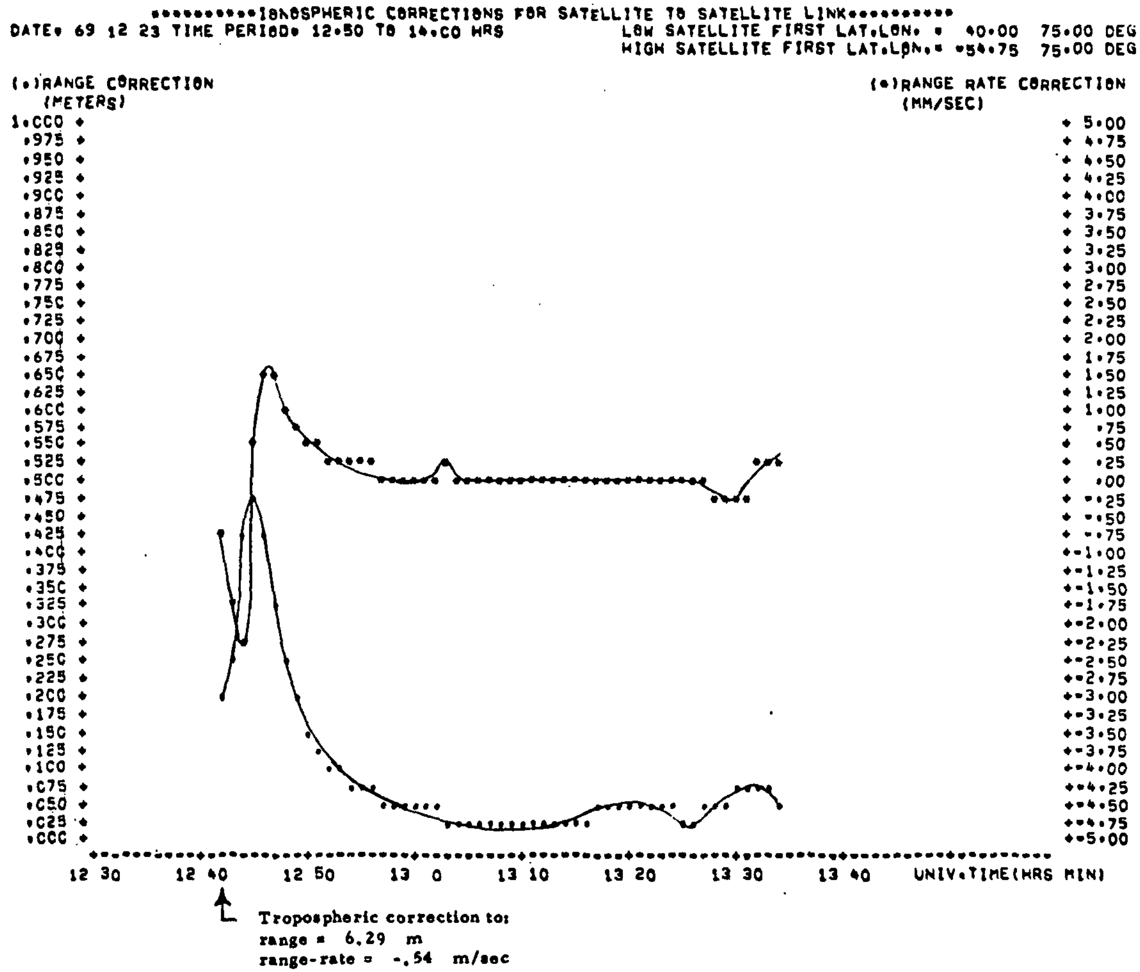
IONOSPHERIC CORRECTIONS FOR SATELLITE TO SATELLITE LINK
DATE, 69 12 23 TIME PERIOD, 12.50 TO 14.CO HRS
LOW SATELLITE FIRST LAT.LON. = 40.00 75.00 DEG
HIGH SATELLITE FIRST LAT.LON.= -54.75 75.00 DEG
(.)RANGE CORRECTION (METERS)
(*)RANGE RATE CORRECTION (MM/SEC)
12 30
12 40
12 50
13 0
13 10
13 20
13 30
13 40
UNIV.TIME(HRS MIN)
Tropospheric correction to:
range = 6.29 m
range-rate = -.54 m/sec

Figure 9h.

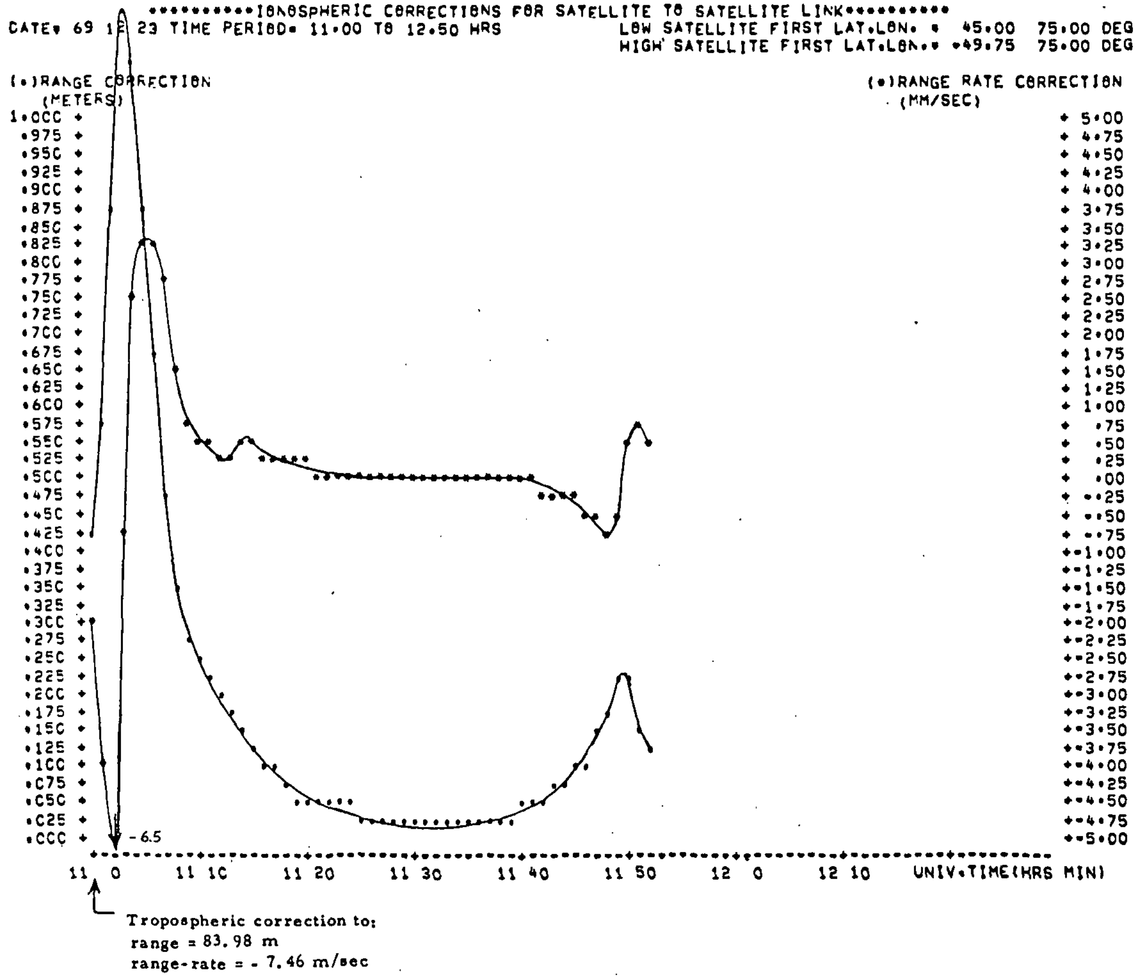
IONOSPHERIC CORRECTIONS FOR SATELLITE TO SATELLITE LINK
DATE, 69 12 23 TIME PERIOD= 11.00 TO 12.50 HRS
LOW SATELLITE FIRST LAT.LON. = 45.00 75.00 DEG
HIGH SATELLITE FIRST LAT.LON.= -49.75 75.00 DEG
(+)RANGE CORRECTION (METERS)
(•)RANGE RATE CORRECTION (MM/SEC)
UNIV.TIME(HRS MIN)
-6.5
Tropospheric correction to:
range = 83.98 m
range-rate = - 7.46 m/sec

Figure 9i.

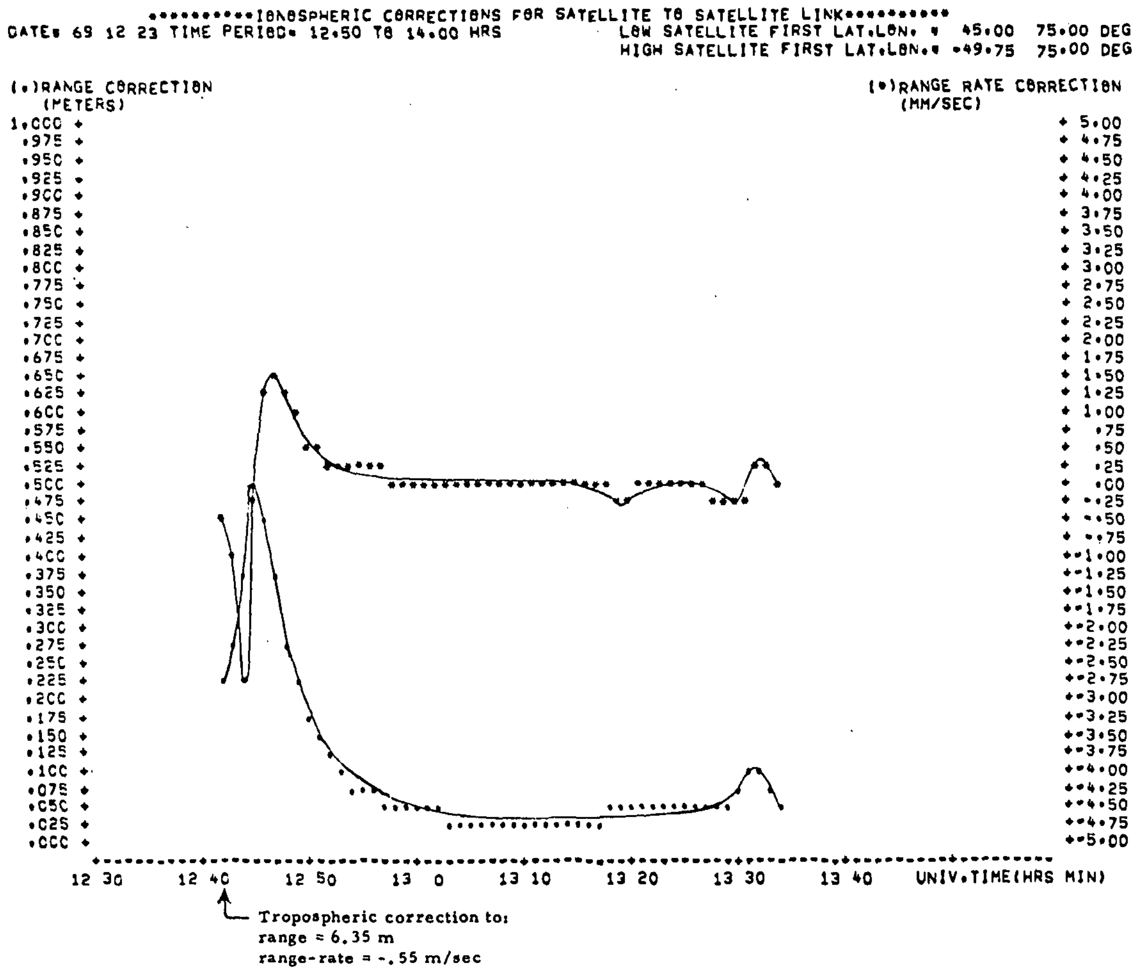
IONOSPHERIC CORRECTIONS FOR SATELLITE TO SATELLITE LINK
DATE= 69 12 23 TIME PERIOD= 12.50 TO 14.00 HRS
LOW SATELLITE FIRST LAT.LON. = 45.00 75.00 DEG
HIGH SATELLITE FIRST LAT.LON. = 49.75 75.00 DEG
(•)RANGE CORRECTION (METERS)
(*)RANGE RATE CORRECTION (MM/SEC)
1.000 .975 .950 .925 .900 .875 .850 .825 .800 .775 .750 .725 .700 .675 .650 .625 .600 .575 .550 .525 .500 .475 .450 .425 .400 .375 .350 .325 .300 .275 .250 .225 .200 .175 .150 .125 .100 .075 .050 .025 .000
5.00 4.75 4.50 4.25 4.00 3.75 3.50 3.25 3.00 2.75 2.50 2.25 2.00 1.75 1.50 1.25 1.00 .75 .50 .25 .00 -.25 -.50 -.75 -1.00 -1.25 -1.50 -1.75 -2.00 -2.25 -2.50 -2.75 -3.00 -3.25 -3.50 -3.75 -4.00 -4.25 -4.50 -4.75 -5.00
12 30 12 40 12 50 13 0 13 10 13 20 13 30 13 40 UNIV.TIME(HRS MIN)
Tropospheric correction to:
range = 6.35 m
range-rate = -.55 m/sec

Figure 9j.

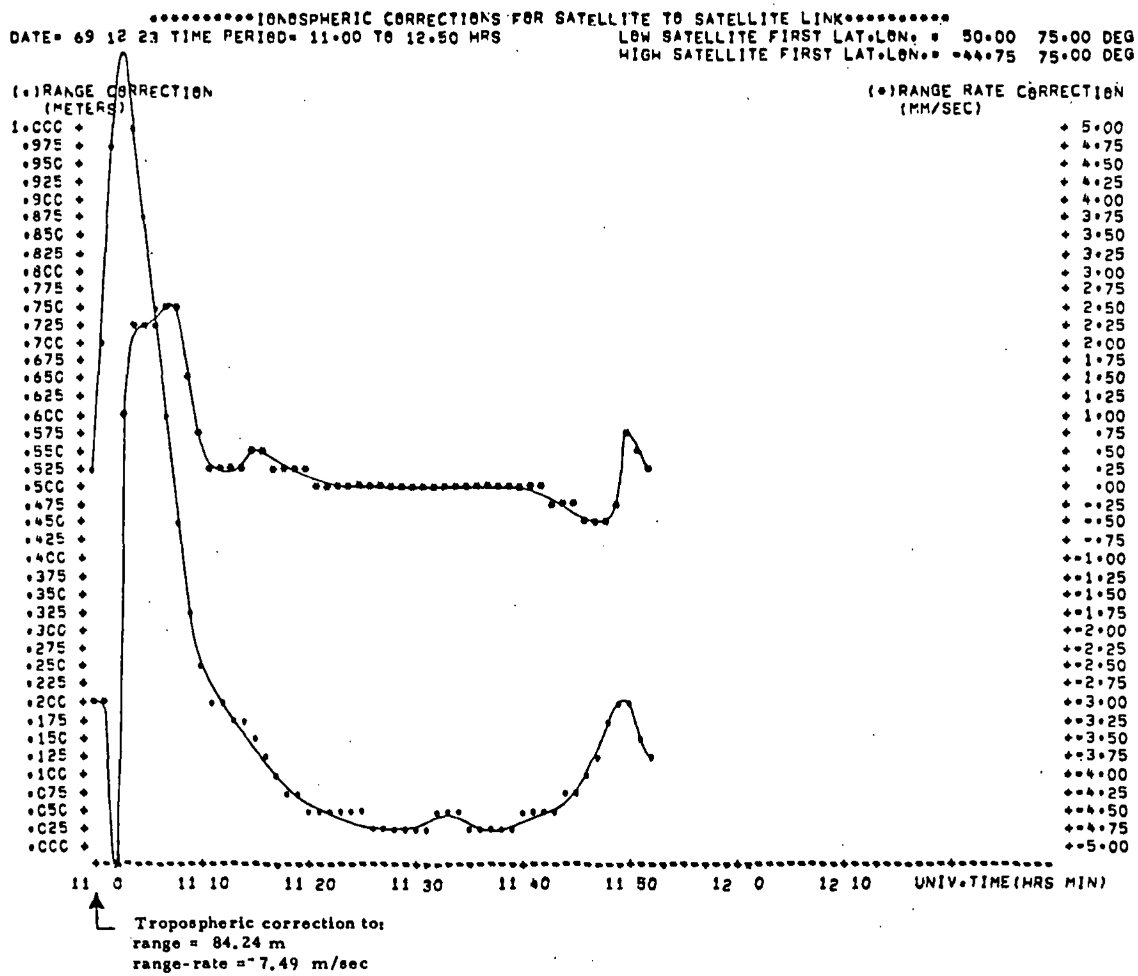
**********IONOSPHERIC CORRECTIONS FOR SATELLITE TO SATELLITE LINK**********
DATE= 69 12 23 TIME PERIOD= 11.00 TO 12.50 HRS
LOW SATELLITE FIRST LAT.LON. = 50.00 75.00 DEG
HIGH SATELLITE FIRST LAT.LON.= -44.75 75.00 DEG
(.)RANGE CORRECTION (METERS)
(*)RANGE RATE CORRECTION (MM/SEC)
1.000 .975 .950 .925 .900 .875 .850 .825 .800 .775 .750 .725 .700 .675 .650 .625 .600 .575 .550 .525 .500 .475 .450 .425 .400 .375 .350 .325 .300 .275 .250 .225 .200 .175 .150 .125 .100 .075 .050 .025 .000
5.00 4.75 4.50 4.25 4.00 3.75 3.50 3.25 3.00 2.75 2.50 2.25 2.00 1.75 1.50 1.25 1.00 .75 .50 .25 .00 -.25 -.50 -.75 -1.00 -1.25 -1.50 -1.75 -2.00 -2.25 -2.50 -2.75 -3.00 -3.25 -3.50 -3.75 -4.00 -4.25 -4.50 -4.75 -5.00
11 0
11 10
11 20
11 30
11 40
11 50
12 0
12 10
UNIV.TIME(HRS MIN)
Tropospheric correction to:
range = 84.24 m
range-rate = -7.49 m/sec

Figure 9k.

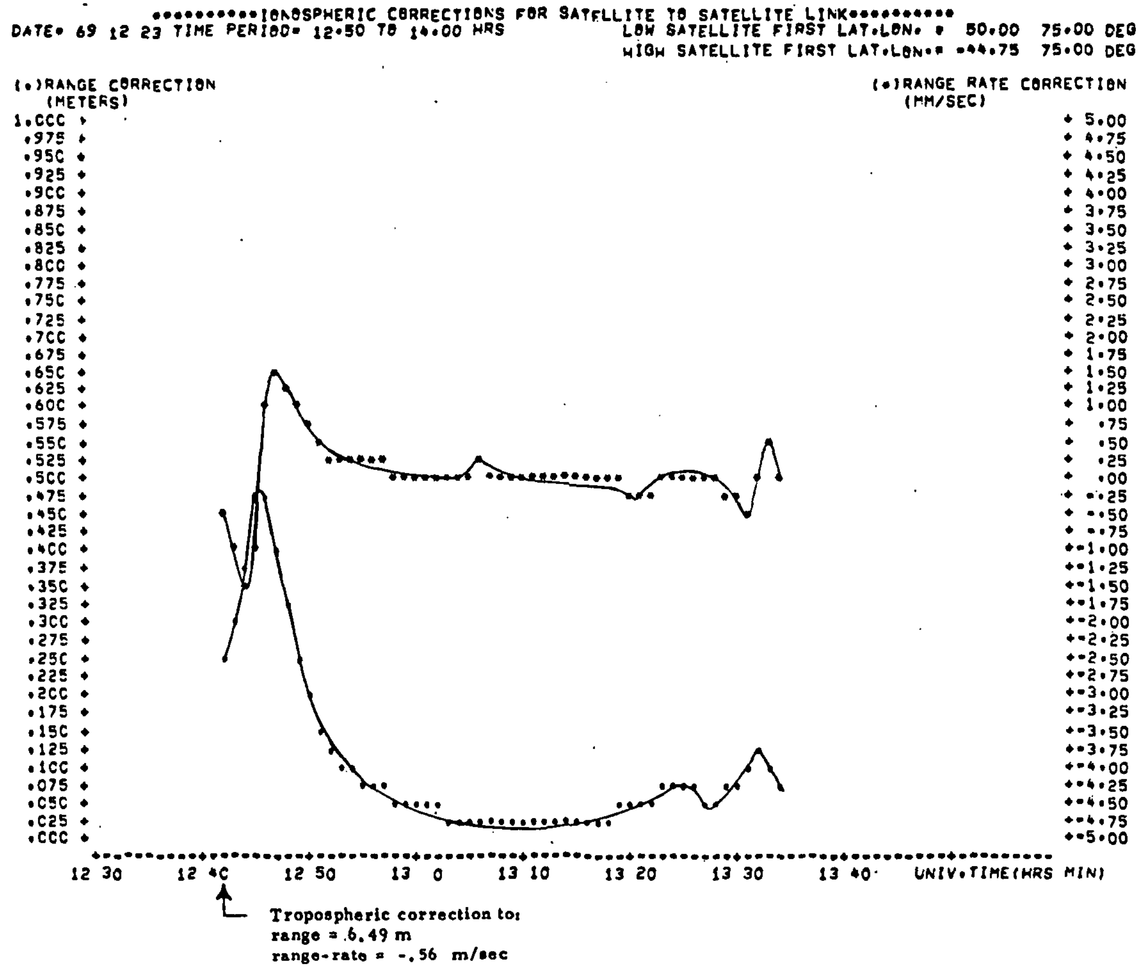
IONOSPHERIC CORRECTIONS FOR SATELLITE TO SATELLITE LINK
DATE= 69 12 23 TIME PERIOD= 12.50 TO 14.00 HRS
LOW SATELLITE FIRST LAT.LON. = 50.00 75.00 DEG
HIGH SATELLITE FIRST LAT.LON.= -44.75 75.00 DEG
(•)RANGE CORRECTION (METERS)
(+)RANGE RATE CORRECTION (MM/SEC)
12 30
12 40
12 50
13 0
13 10
13 20
13 30
13 40
UNIV.TIME(HRS MIN)
Tropospheric correction to:
range = 6.49 m
range-rate = -.56 m/sec

Figure 91.

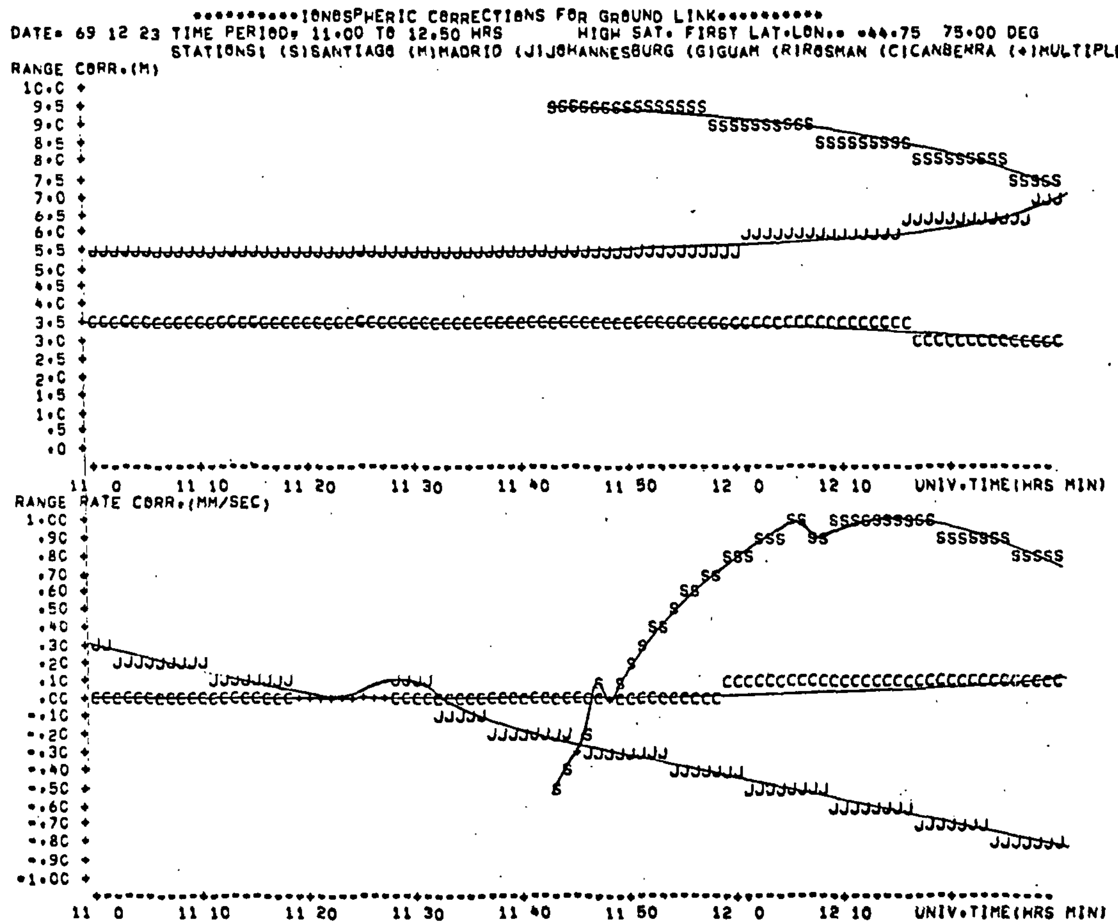
**********IONOSPHERIC CORRECTIONS FOR GROUND LINK**********
DATE= 69 12 23 TIME PERIOD= 11.00 TO 12.50 HRS HIGH SAT. FIRST LAT.LON.= =44.75 75.00 DEG
STATIONS: (S)SANTIAGO (M)MADRID (J)JOHANNESBURG (G)GUAM (R)ROSMAN (C)CANBERRA (+)MULTIPLE
RANGE CORR.(M)
RANGE RATE CORR.(MM/SEC)
11 0
11 10
11 20
11 30
11 40
11 50
12 0
12 10
UNIV.TIME(HRS MIN)

Figure 10a.

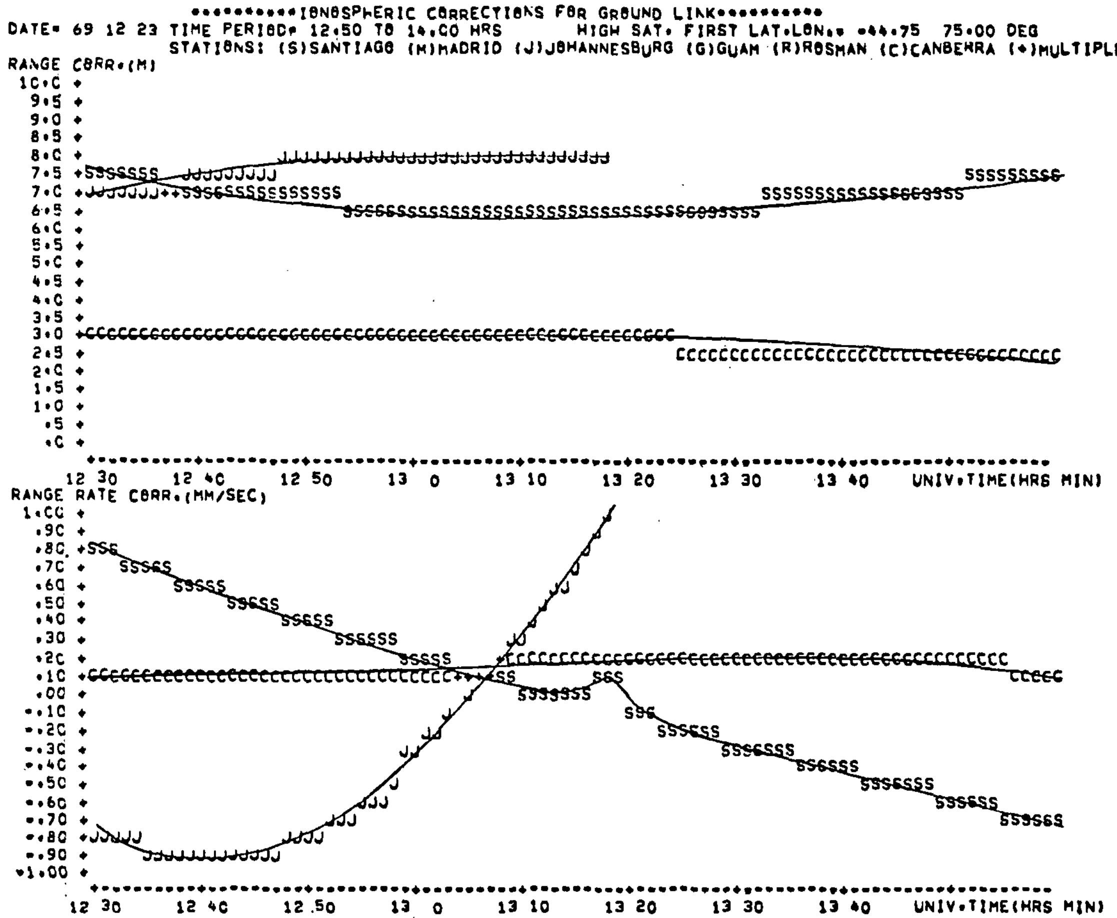
IONOSPHERIC CORRECTIONS FOR GROUND LINK
DATE= 69 12 23 TIME PERIOD= 12.50 TO 14.00 HRS HIGH SAT. FIRST LAT.LON.= -44.75 75.00 DEG
STATIONS: (S)SANTIAGO (M)MADRID (J)JOHANNESBURG (G)GUAM (R)ROSMAN (C)CANBERRA (+)MULTIPLE
RANGE CORR.(M)
UNIV.TIME(HRS MIN)
RANGE RATE CORR.(MM/SEC)
UNIV.TIME(HRS MIN)

Figure 10b.

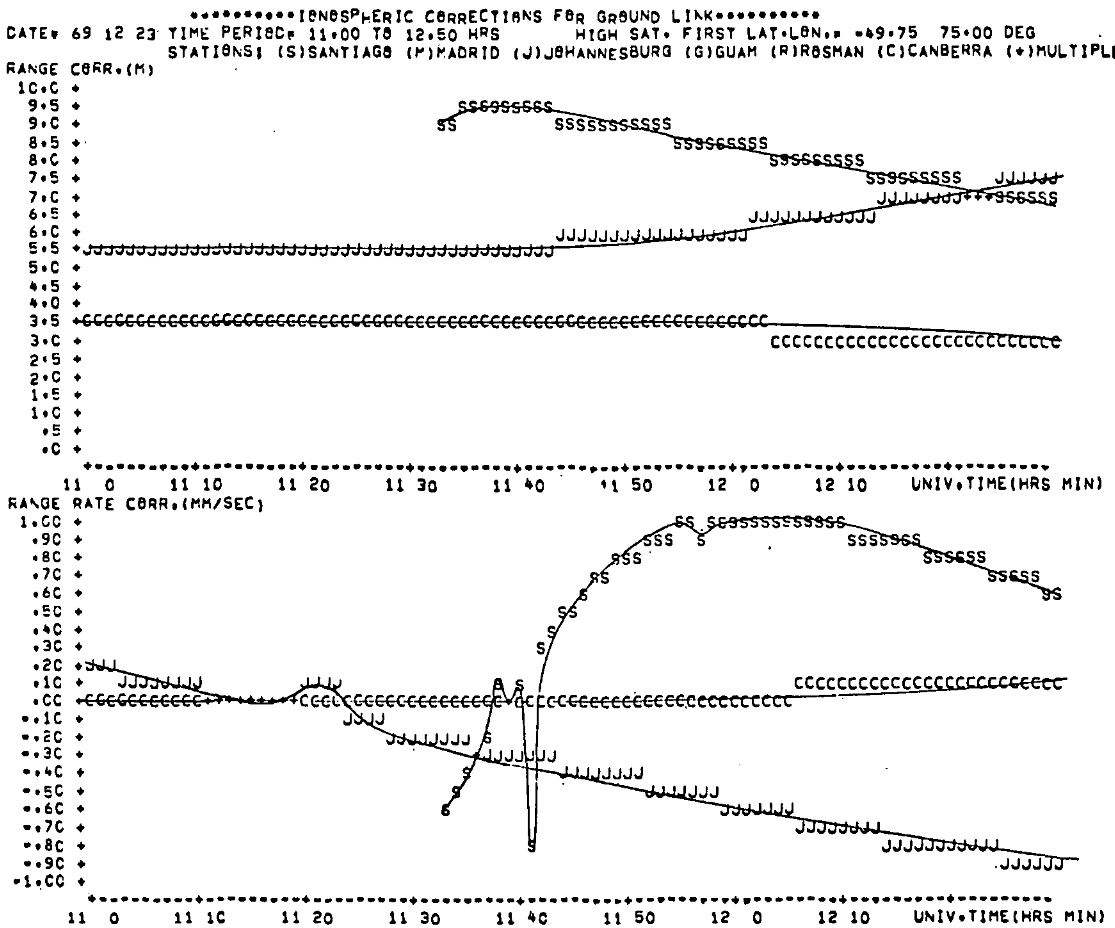
**********IONOSPHERIC CORRECTIONS FOR GROUND LINK**********
DATE= 69 12 23 TIME PERIOD= 11.00 TO 12.50 HRS HIGH SAT. FIRST LAT.LON.= -49.75 75.00 DEG
STATIONS: (S)SANTIAGO (M)MADRID (J)JOHANNESBURG (G)GUAM (R)ROSMAN (C)CANBERRA (+)MULTIPLE
RANGE CORR.(M)
UNIV.TIME(HRS MIN)
RANGE RATE CORR.(MM/SEC)
UNIV.TIME(HRS MIN)

Figure 10c.

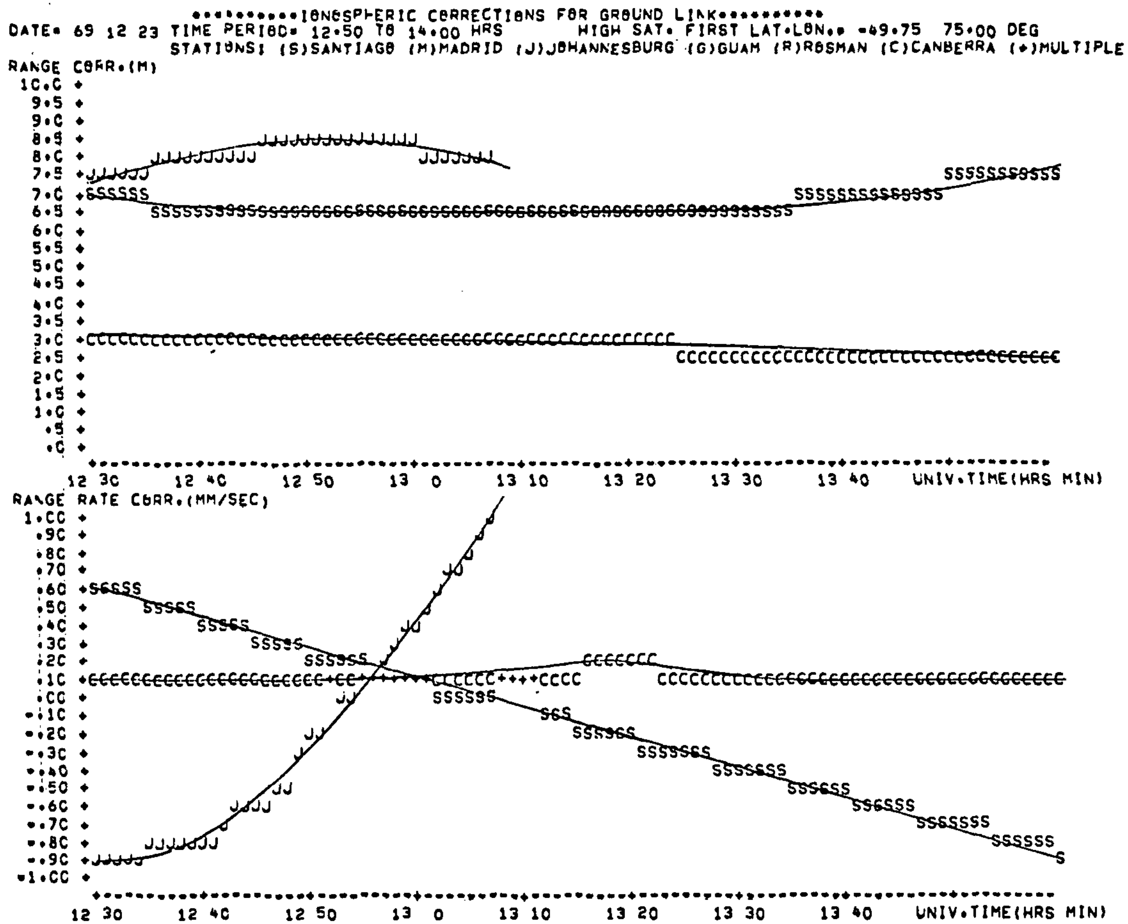
IONOSPHERIC CORRECTIONS FOR GROUND LINK
DATE= 69 12 23 TIME PERIOD= 12.50 TO 14.00 HRS HIGH SAT. FIRST LAT.LON.= -49.75 75.00 DEG
STATIONS: (S)SANTIAGO (M)MADRID (J)JOHANNESBURG (G)GUAM (R)ROSMAN (C)CANBERRA (+)MULTIPLE
RANGE CORR.(M)
RANGE RATE CORR.(MM/SEC)
UNIV.TIME(HRS MIN)

Figure 10d.

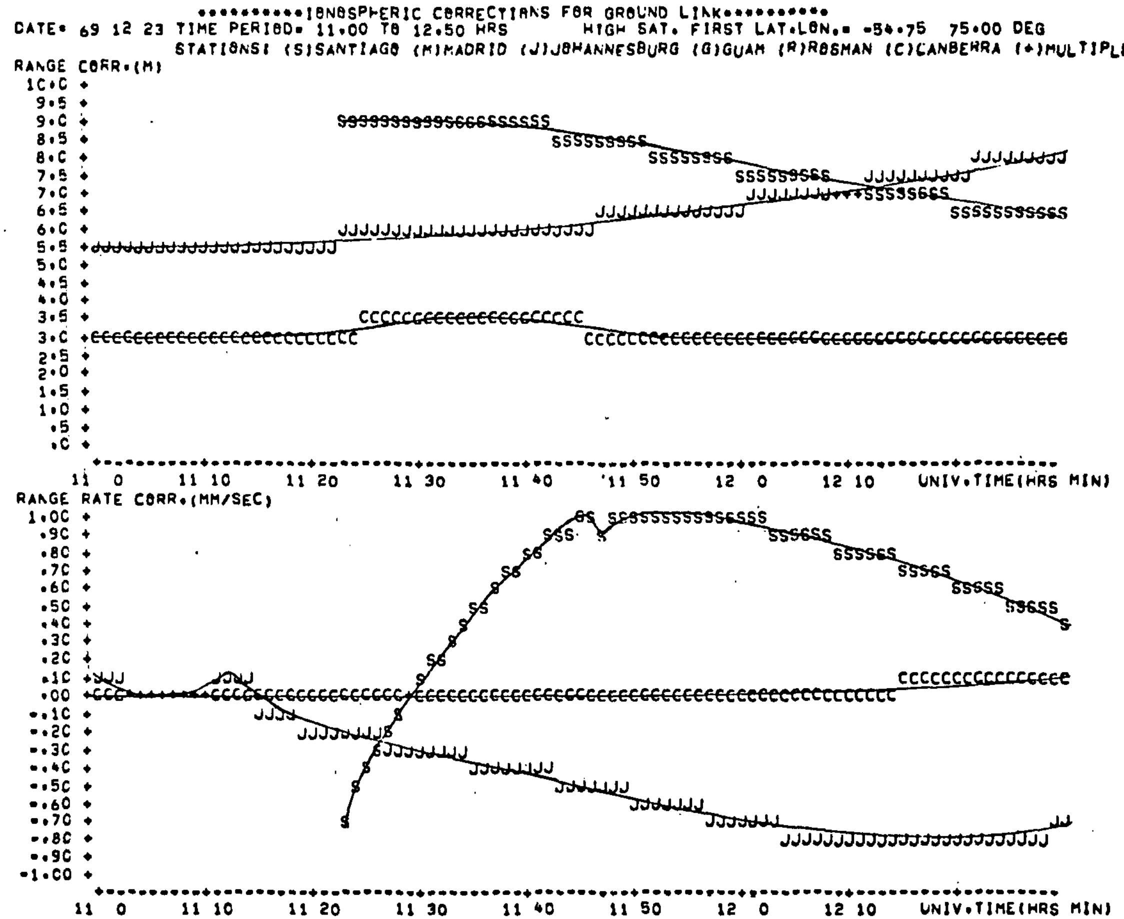

**********IONOSPHERIC CORRECTIONS FOR GROUND LINK**********
DATE= 69 12 23 TIME PERIOD= 11.00 TO 12.50 HRS HIGH SAT. FIRST LAT.LON.= -54.75 75.00 DEG
STATIONS: (S)SANTIAGO (M)MADRID (J)JOHANNESBURG (G)GUAM (R)ROSMAN (C)CANBERRA (+)MULTIPLE
RANGE CORR.(M)
UNIV.TIME(HRS MIN)
RANGE RATE CORR.(MM/SEC)
UNIV.TIME(HRS MIN)

Figure 10e.

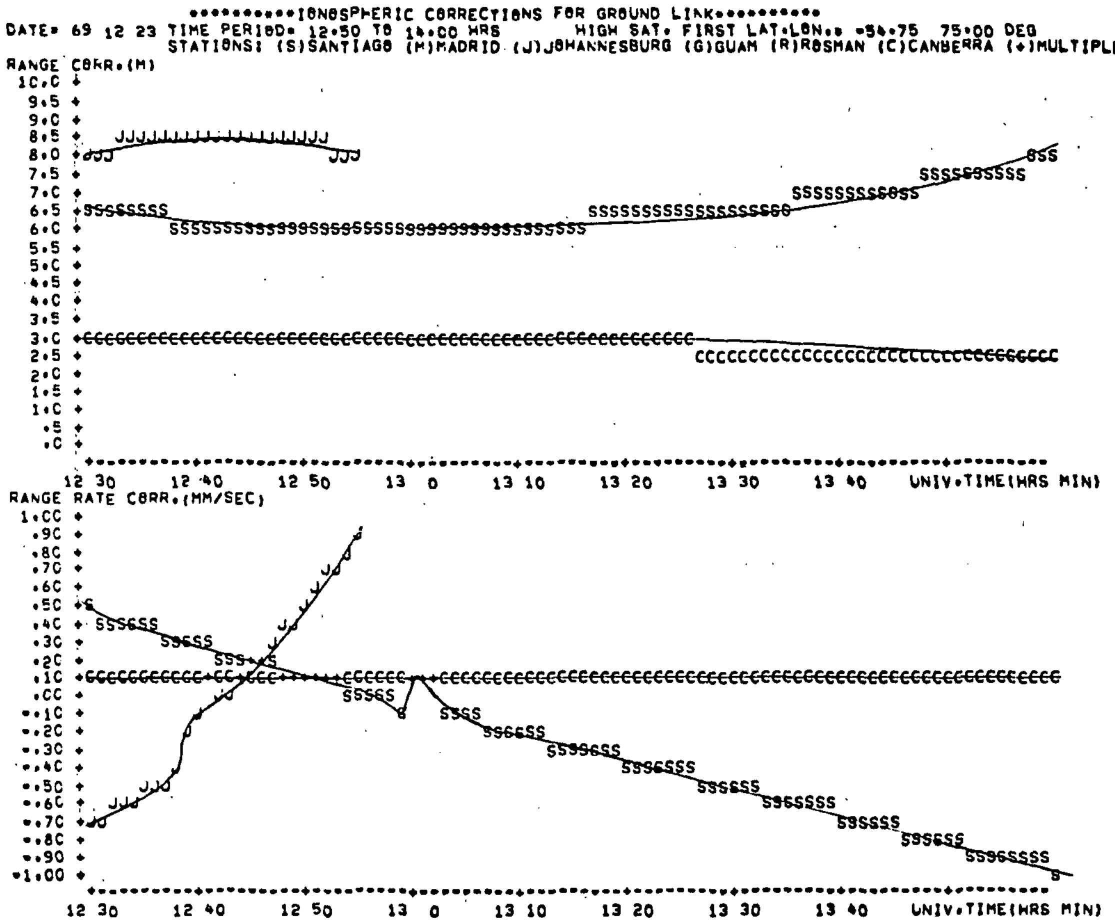
IONOSPHERIC CORRECTIONS FOR GROUND LINK
DATE= 69 12 23 TIME PERIOD= 12.50 TO 14.00 HRS
HIGH SAT. FIRST LAT.LON.= -54.75 75.00 DEG
STATIONS: (S)SANTIAGO (M)MADRID (J)JOHANNESBURG (G)GUAM (R)ROSMAN (C)CANBERRA (+)MULTIPLE
RANGE CORR.(M)
12 30
12 40
12 50
13 0
13 10
13 20
13 30
13 40
UNIV.TIME(HRS MIN)
RANGE RATE CORR.(MM/SEC)

Figure 10f.

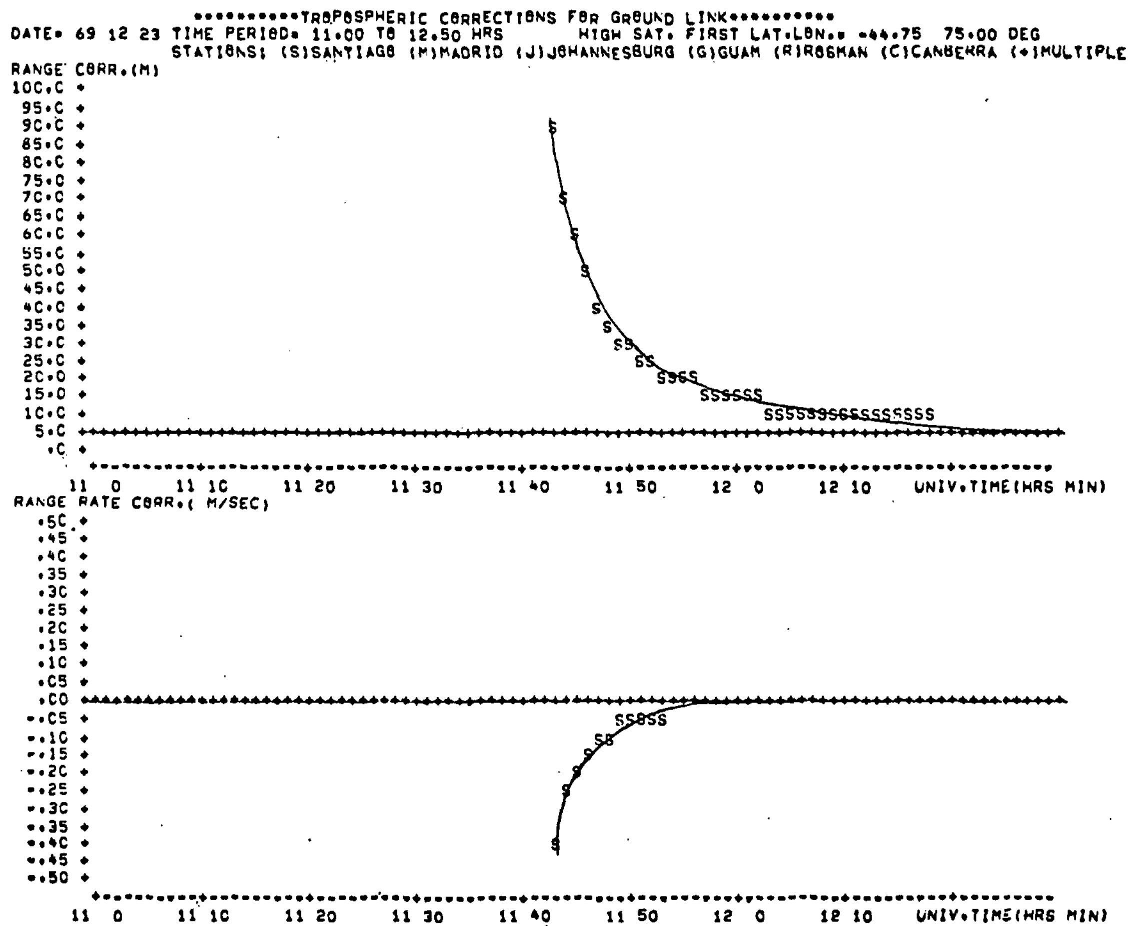
***********TROPOSPHERIC CORRECTIONS FOR GROUND LINK***********
DATE= 69 12 23 TIME PERIOD= 11.00 TO 12.50 HRS HIGH SAT. FIRST LAT.LON.= -44.75 75.00 DEG
STATIONS: (S)SANTIAGO (M)MADRID (J)JOHANNESBURG (G)GUAM (R)ROSMAN (C)CANBERRA (+)MULTIPLE
RANGE CORR.(M)
100.0
95.0
90.0
85.0
80.0
75.0
70.0
65.0
60.0
55.0
50.0
45.0
40.0
35.0
30.0
25.0
20.0
15.0
10.0
5.0
.0
11 0
11 10
11 20
11 30
11 40
11 50
12 0
12 10
UNIV.TIME(HRS MIN)
RANGE RATE CORR.(M/SEC)
.50
.45
.40
.35
.30
.25
.20
.15
.10
.05
.00
-.05
-.10
-.15
-.20
-.25
-.30
-.35
-.40
-.45
-.50
11 0
11 10
11 20
11 30
11 40
11 50
12 0
12 10
UNIV.TIME(HRS MIN)

Figure 11a.

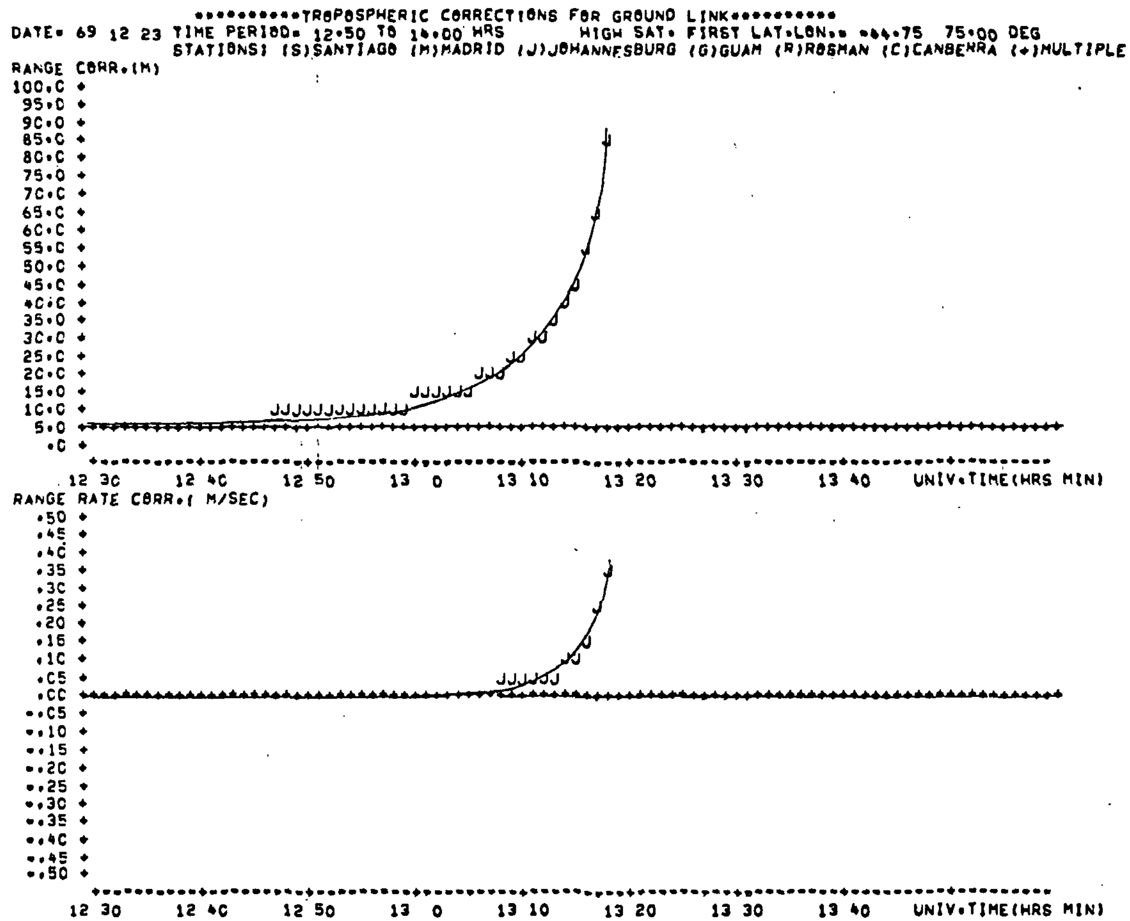
TROPOSPHERIC CORRECTIONS FOR GROUND LINK
DATE= 69 12 23 TIME PERIOD= 12.50 TO 14.00 HRS HIGH SAT. FIRST LAT.LON.= -64.75 75.00 DEG
STATIONS: (S)SANTIAGO (M)MADRID (J)JOHANNESBURG (G)GUAM (R)ROSMAN (C)CANBERRA (+)MULTIPLE
RANGE CORR.(M)
RANGE RATE CORR.(M/SEC)
12 30
12 40
12 50
13 0
13 10
13 20
13 30
13 40
UNIV.TIME(HRS MIN)

Figure 11b.

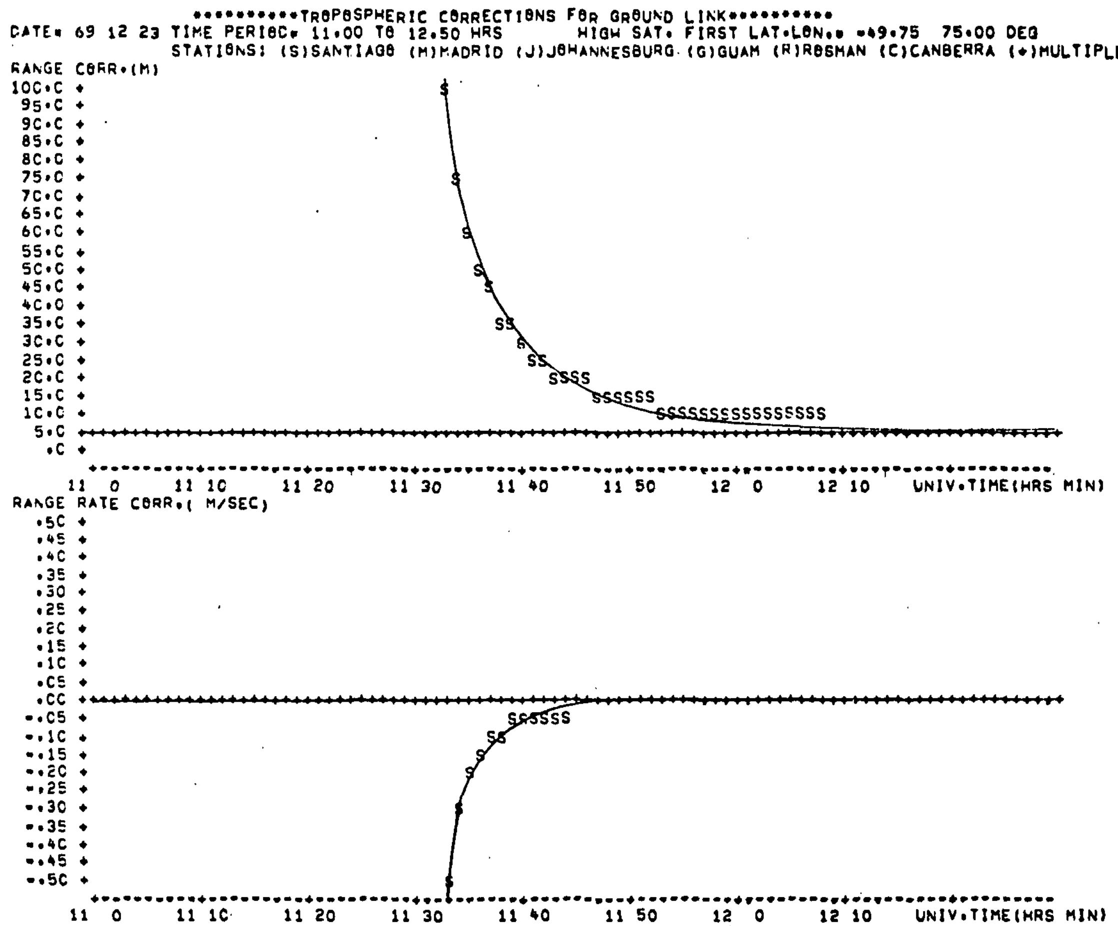
**********TROPOSPHERIC CORRECTIONS FOR GROUND LINK**********
DATE= 69 12 23 TIME PERIOD= 11.00 TO 12.50 HRS
HIGH SAT. FIRST LAT.LON.= -49.75 75.00 DEG
STATIONS: (S)SANTIAGO (M)MADRID (J)JOHANNESBURG (G)GUAM (R)ROSMAN (C)CANBERRA (+)MULTIPLE
RANGE CORR.(M)
100.0
95.0
90.0
85.0
80.0
75.0
70.0
65.0
60.0
55.0
50.0
45.0
40.0
35.0
30.0
25.0
20.0
15.0
10.0
5.0
.0
11 0
11 10
11 20
11 30
11 40
11 50
12 0
12 10
UNIV.TIME(HRS MIN)
RANGE RATE CORR.(M/SEC)
.50
.45
.40
.35
.30
.25
.20
.15
.10
.05
.00
-.05
-.10
-.15
-.20
-.25
-.30
-.35
-.40
-.45
-.50
11 0
11 10
11 20
11 30
11 40
11 50
12 0
12 10
UNIV.TIME(HRS MIN)

Figure 11c.

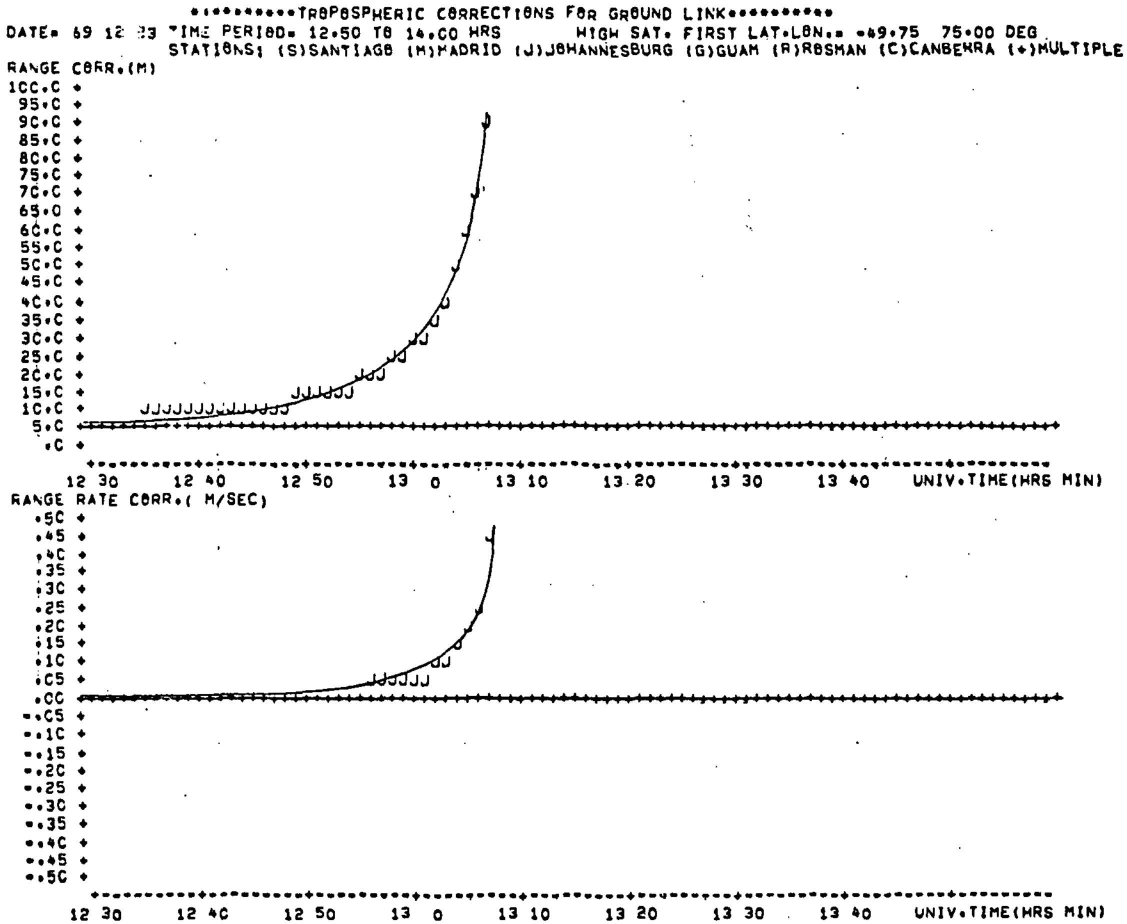
TROPOSPHERIC CORRECTIONS FOR GROUND LINK
DATE= 69 12 23 TIME PERIOD= 12.50 TO 14.00 HRS HIGH SAT. FIRST LAT.LON.= -49.75 75.00 DEG
STATIONS; (S)SANTIAGO (M)MADRID (J)JOHANNESBURG (G)GUAM (R)ROSMAN (C)CANBERRA (+)MULTIPLE
RANGE CORR.(M)
100.0
95.0
90.0
85.0
80.0
75.0
70.0
65.0
60.0
55.0
50.0
45.0
40.0
35.0
30.0
25.0
20.0
15.0
10.0
5.0
.0
12 30
12 40
12 50
13 0
13 10
13 20
13 30
13 40
UNIV.TIME(HRS MIN)
RANGE RATE CORR.(M/SEC)
.50
.45
.40
.35
.30
.25
.20
.15
.10
.05
.00
-.05
-.10
-.15
-.20
-.25
-.30
-.35
-.40
-.45
-.50
12 30
12 40
12 50
13 0
13 10
13 20
13 30
13 40
UNIV.TIME(HRS MIN)

Figure 11d.

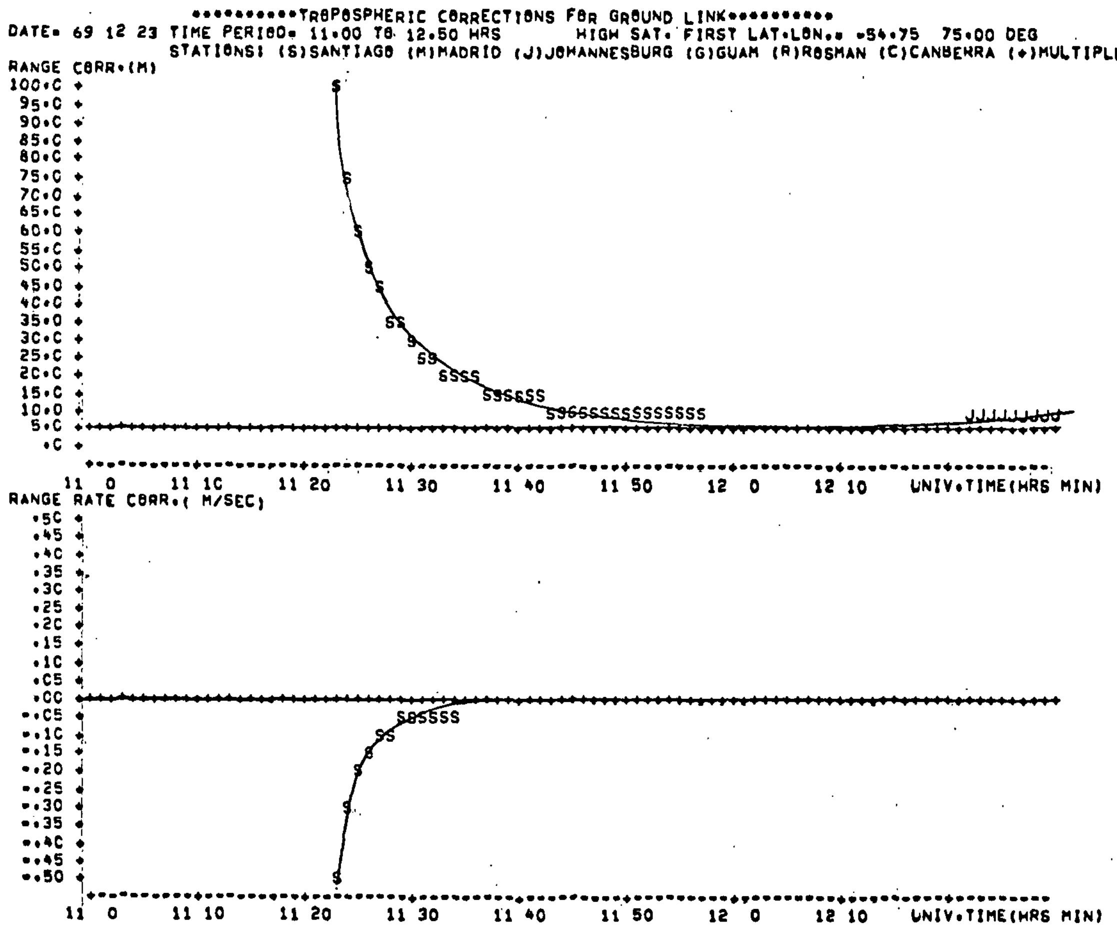
TROPOSPHERIC CORRECTIONS FOR GROUND LINK
DATE= 69 12 23 TIME PERIOD= 11.00 TO 12.50 HRS HIGH SAT. FIRST LAT.LON.= -54.75 75.00 DEG
STATIONS: (S)SANTIAGO (M)MADRID (J)JOHANNESBURG (G)GUAM (R)ROSMAN (C)CANBERRA (+)MULTIPLE
RANGE CORR.(M)
100.0 95.0 90.0 85.0 80.0 75.0 70.0 65.0 60.0 55.0 50.0 45.0 40.0 35.0 30.0 25.0 20.0 15.0 10.0 5.0 .0
11 0 11 10 11 20 11 30 11 40 11 50 12 0 12 10 UNIV.TIME(HRS MIN)
RANGE RATE CORR.(M/SEC)
.50 .45 .40 .35 .30 .25 .20 .15 .10 .05 .00 -.05 -.10 -.15 -.20 -.25 -.30 -.35 -.40 -.45 -.50
11 0 11 10 11 20 11 30 11 40 11 50 12 0 12 10 UNIV.TIME(HRS MIN)

Figure 11e.

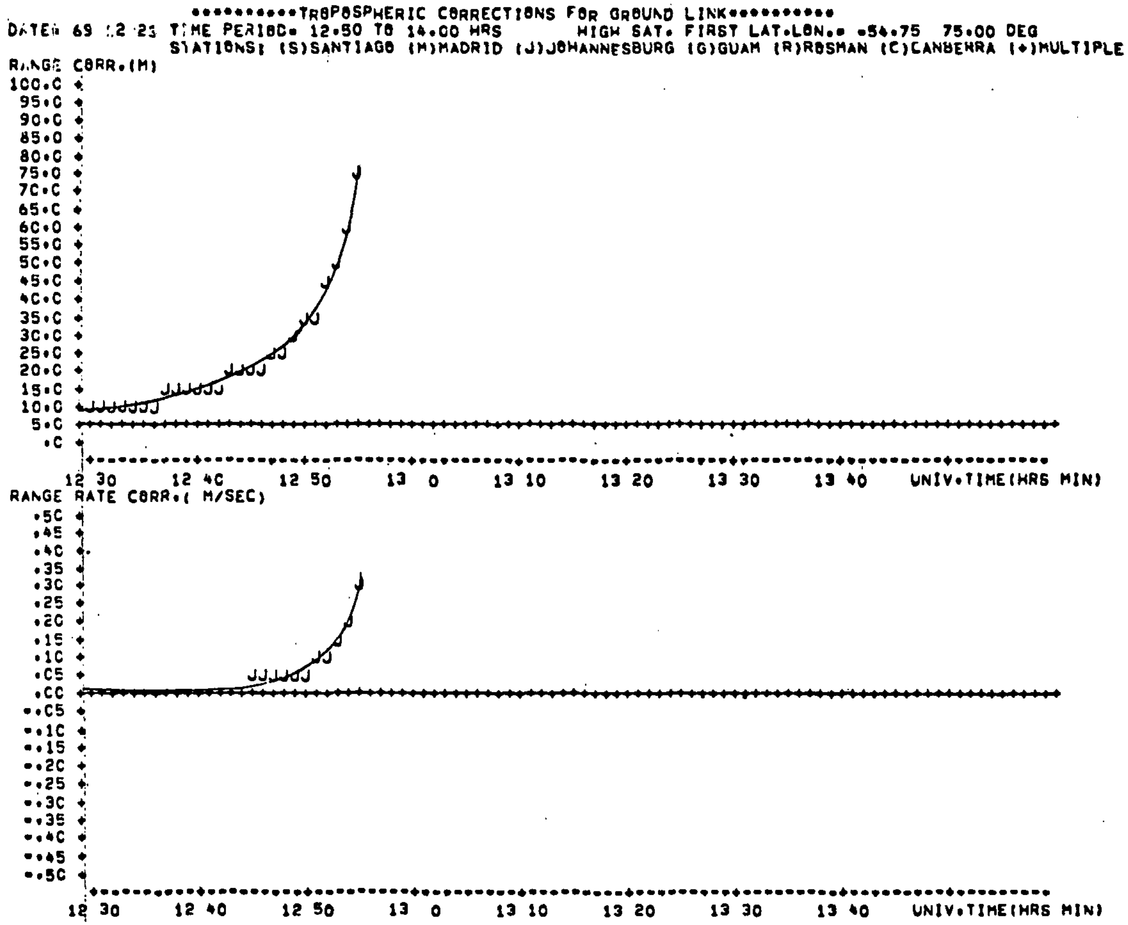
**********TROPOSPHERIC CORRECTIONS FOR GROUND LINK**********
DATE: 69 12 23 TIME PERIOD= 12.50 TO 14.00 HRS HIGH SAT. FIRST LAT.LON.= -54.75 75.00 DEG
STATIONS: (S)SANTIAGO (M)MADRID (J)JOHANNESBURG (G)GUAM (R)ROSMAN (C)CANBERRA (+)MULTIPLE
RANGE CORR.(M)
100.0
95.0
90.0
85.0
80.0
75.0
70.0
65.0
60.0
55.0
50.0
45.0
40.0
35.0
30.0
25.0
20.0
15.0
10.0
5.0
.0
12 30
12 40
12 50
13 0
13 10
13 20
13 30
13 40
UNIV.TIME(HRS MIN)
RANGE RATE CORR.(M/SEC)
.50
.45
.40
.35
.30
.25
.20
.15
.10
.05
.00
-.05
-.10
-.15
-.20
-.25
-.30
-.35
-.40
-.45
-.50
12 30
12 40
12 50
13 0
13 10
13 20
13 30
13 40
UNIV.TIME(HRS MIN)

Figure 11f.

7.0 REFERENCES

1. J. W. Marini, "Closed Form Satellite Tracking Data Corrections for an Arbitrary Tropospheric Profile", NASA Document X-551-71-122, March 1971

2. S. K. Llewellyn, R. B. Bent, "Documentation and Description of the Bent Ionospheric Model", AFCRL-TR-73-0657, SAMSO TR-73-252, July 1973

NASA-Langley, 1977

"The aeronautical and space activities of the United States shall be conducted so as to contribute . . . to the expansion of human knowledge of phenomena in the atmosphere and space. The Administration shall provide for the widest practicable and appropriate dissemination of information concerning its activities and the results thereof."

—NATIONAL AERONAUTICS AND SPACE ACT OF 1958

NASA SCIENTIFIC AND TECHNICAL PUBLICATIONS

TECHNICAL REPORTS: Scientific and technical information considered important, complete, and a lasting contribution to existing knowledge.

TECHNICAL NOTES: Information less broad in scope but nevertheless of importance as a contribution to existing knowledge.

TECHNICAL MEMORANDUMS: Information receiving limited distribution because of preliminary data, security classification, or other reasons. Also includes conference proceedings with either limited or unlimited distribution.

CONTRACTOR REPORTS: Scientific and technical information generated under a NASA contract or grant and considered an important contribution to existing knowledge.

TECHNICAL TRANSLATIONS: Information published in a foreign language considered to merit NASA distribution in English.

SPECIAL PUBLICATIONS: Information derived from or of value to NASA activities. Publications include final reports of major projects, monographs, data compilations, handbooks, sourcebooks, and special bibliographies.

TECHNOLOGY UTILIZATION PUBLICATIONS: Information on technology used by NASA that may be of particular interest in commercial and other non-aerospace applications. Publications include Tech Briefs, Technology Utilization Reports and Technology Surveys.

Details on the availability of these publications may be obtained from:

SCIENTIFIC AND TECHNICAL INFORMATION OFFICE

NATIONAL AERONAUTICS AND SPACE ADMINISTRATION

Washington, D.C. 20546